polysaccharides

MDPI

Article

Decoding the Bioactive Potential of Blackcurrant Pomace Extract: Toward Biofunctional and Skin-Comfortable Polysaccharide-Based Textiles

Aleksandra Ivanovska [1,*], Marija Ćorović [2], Anja Petrov Ivanković [1], Tanja Lunić [3], Anita Tarbuk [4], Xiang-Kui Ren [5,6] and Igor Jordanov [7]

[1] Innovation Center of the Faculty of Technology and Metallurgy, University of Belgrade, Karnegijeva 4, 11000 Belgrade, Serbia; apetrov@tmf.bg.ac.rs
[2] Faculty of Technology and Metallurgy, University of Belgrade, Karnegijeva 4, 11000 Belgrade, Serbia; mstojanovic@tmf.bg.ac.rs
[3] Faculty of Biology, Institute of Physiology and Biochemistry "Ivan Đaja", University of Belgrade, Studentski Trg 16, 11000 Belgrade, Serbia; tanja.lunic@bio.bg.ac.rs
[4] Faculty of Textile Technology, University of Zagreb, Prilaz baruna Filipovića 28a, 10000 Zagreb, Croatia; anita.tarbuk@ttf.unizg.hr
[5] School of Chemical Engineering and Technology, Tianjin University, Tianjin 300350, China; renxiangkui@tju.edu.cn
[6] Zhejiang Institute of Tianjin University, Ningbo 315200, China
[7] Faculty of Technology and Metallurgy, Ss. Cyril and Methodius University in Skopje, Ruger Boskovic 16, 1000 Skopje, North Macedonia; jordanov@tmf.ukim.edu.mk
* Correspondence: aivanovska@tmf.bg.ac.rs; Tel.: +381-11-330-3628

Abstract

This study presents a novel approach for the development of biofunctional and skin-comfortable cotton textiles through the integration of blackcurrant water/ethanol pomace extract into polysaccharide-based fabric coating. Extraction of bioactive compounds from blackcurrant pomace was optimized using response surface methodology, yielding a total phenolic content of 36.04 mg GAE/g DW, along with significant contents of flavonoids (5.28 mg QE/g DW) and anthocyanins (5.18 mg/g DW). The cotton fabric was biofunctionalized using the layer-by-layer (LbL) deposition technique, incorporating blackcurrant pomace extract within four, eight, or twelve chitosan/pectin bilayers. The biofunctionalized fabrics exhibited no cytotoxic effect and demonstrated nearly 100% antioxidant and antibacterial activity against *E. coli* and *S. aureus*. Additionally, the LbL coating enabled tunable extract adsorption (0.09–2.70%) and stabilization of bioactive compounds on the cotton surface, resulting in adjustable fabric coloration and moisture management properties (assessed using the Moisture Management Tester). Molecular docking analysis provided insight into the interactions between HPLC-detected anthocyanins (cyanidin-3-O-glucoside, cyanidin-3-O-rutinoside, delphinidin-3-O-glucoside, and delphinidin-3-O-rutinoside) and polysaccharides, revealing an increase in binding affinity from cellulose to chitosan and pectin. The transition from comfort-oriented fabric to a material featuring integrated moisture management and enhanced biofunctionality, achieved by coating cotton with eight chitosan/pectin bilayers incorporating blackcurrant pomace extract, renders the textile suited for medical, protective, and high-comfort applications.

Keywords: blackcurrant; pomace; extract; polysaccharide; cotton; chitosan; pectin; layer-by-layer; functionalization; comfort

Check for updates

Academic Editors: Tina Maver and Uroš Maver

Received: 5 May 2026
Revised: 2 June 2026
Accepted: 15 June 2026
Published: 18 June 2026

Copyright: © 2026 by the authors. Licensee MDPI, Basel, Switzerland. This article is an open access article distributed under the terms and conditions of the Creative Commons Attribution (CC BY) license.

1. Introduction

The global demand for advanced textiles with different functionalities has increased markedly in recent years, driven by growing concerns related to health, hygiene, and environmental sustainability. Within this context, biofunctional textiles represent a prominent and rapidly expanding category, accounting for approximately 7% of the total functional textile market [1]. Biofunctional textiles are materials engineered through the incorporation of bioactive agents or via surface modification strategies to impart specific bioactive functions, thereby enabling interactions with the human body to enhance health, hygiene, therapeutic efficacy, and overall well-being [2–4]. Such textiles exhibit the ability to inhibit microbial proliferation and mitigate oxidative stress, which underpins their increasing utilization in medical garments and hospital linens, where they contribute to infection control [5,6]. Furthermore, biofunctional textiles have gained considerable attention due to their capacity to act as active delivery systems, either by absorbing substances from the skin or by releasing therapeutic and cosmetic agents in a controlled manner, thereby expanding their applicability in both medical and personal care domains [7].

Chemicals conventionally employed to impart biofunctional properties to textiles are predominantly synthetic and are frequently associated with varying degrees of toxicity, as well as reduced long-term efficacy due to their extensive use and the consequent development of microbial resistance [3]. Natural substances, particularly those exhibiting antimicrobial and antioxidant properties, have therefore emerged as attractive candidates for biofunctional textile applications. Extracts derived from plant, fruit, and animal sources are increasingly favored as renewable and biocompatible sources of functional biomolecules [8]. Nevertheless, challenges related to the limited stability of natural extracts and their efficient integration into textiles remain significant, thereby necessitating the development of alternative strategies to enhance both the stability of bioactive compounds and the efficiency of textile functionalization.

These objectives can be achieved through the implementation of tailored textile finishing technologies, such as padding, spraying, and layer-by-layer deposition, or alternatively by enhancing the adsorption of extract bioactive agents through the establishment of weak intermolecular interactions with the textile substrate [5,9]. Among these, the layer-by-layer approach has emerged as a particularly effective method for increasing the loading capacity of extracted bioactive compounds onto fabric surfaces. Precisely, this technique is based on the sequential deposition of oppositely charged layers, which enables the efficient incorporation of bioactive compounds within each deposited layer. Polysaccharides such as chitosan and pectin have demonstrated a strong capacity to interact with and retain bioactive molecules, making them suitable candidates for enhancing extract loading and its stability on the textile surface [10,11].

In this study, cotton was selected as the substrate for the development of polysaccharide-based biofunctional textiles due to its excellent comfort, high biocompatibility, and good wettability, which facilitates its functionalization via wet finishing processes [5]. Moreover, cotton is widely used in applications involving individuals with contact dermatitis and other skin-related conditions, owing to its superior moisture management properties [12]. Based on prior experimental experience and the aforementioned studies, cotton fabrics were functionalized using a layer-by-layer deposition of chitosan/pectin bilayers incorporating a water/ethanol extract of blackcurrant pomace. Blackcurrant pomace, a major by-product of the fruit juice industry, was selected as a sustainable source of bioactive compounds due to its high content of phenolic compounds, particularly anthocyanins, which are known for their antioxidant, antimicrobial, anti-inflammatory, antiviral, regenerative, and anti-aging properties [13,14]. To maximize the recovery of bioactive compounds from blackcurrant pomace, extraction was performed using ethanol of various concentrations due to its wide

recognition as a highly effective solvent for the extraction of phenolic compounds and anthocyanins from plant-based materials. After the optimization of the bioactive compound extraction with respect to total phenolic content, the flavonoid content was determined, and the most abundant anthocyanins in the optimized blackcurrant pomace extract were identified and quantified by HPLC. The optimized extract was added to chitosan or pectin solutions and applied to cotton fabrics through layer-by-layer deposition using 4, 8, or 12 polysaccharide bilayers. After functionalization, the antioxidant and antibacterial activities, as well as cytotoxicity and pH of aqueous extract of coated fabrics, were evaluated to confirm their biofunctionality and to identify the most effective functionalization protocol. In addition to their bioactivity, blackcurrant pomace extracts are known to impart aesthetically desirable coloration to textile substrates; therefore, the color properties of the functionalized fabrics were also assessed. Furthermore, considering that the practical applicability and market potential of biofunctional textiles are strongly dependent on user comfort [15], particular attention was devoted to the evaluation of moisture management properties and contact angle in order to assess the skin comfort and wettability characteristics of the developed biofunctional fabrics. Importantly, molecular docking analysis was employed to elucidate the interactions between the major extract anthocyanins and the polysaccharide components (cellulose, chitosan, and pectin), providing mechanistic insight into the enhanced stability of bioactive compounds on the cotton surface. The overall novelty of this study is summarized in Figure 1.

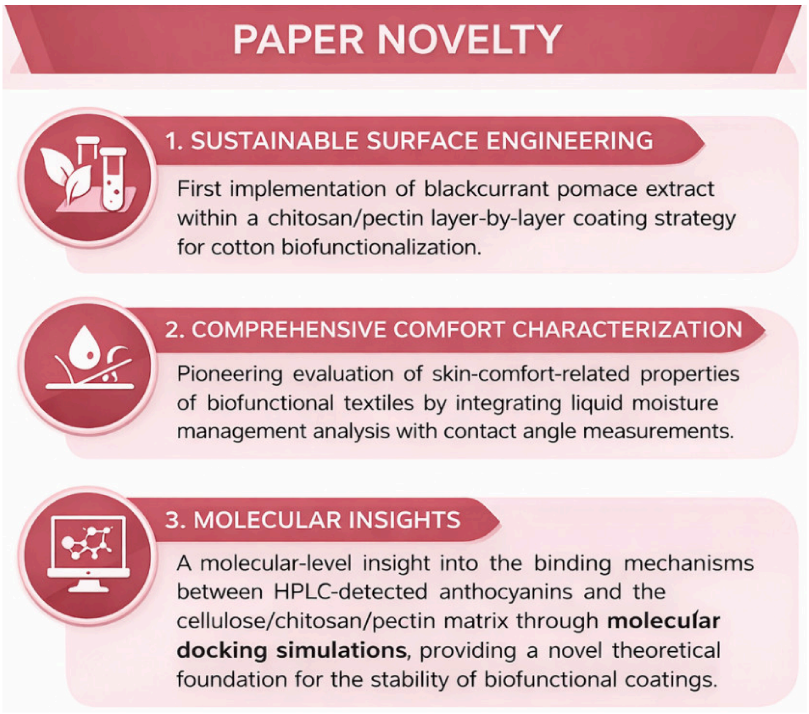


Figure 1. Key novelties of the study.

The integration of biotechnology with textile engineering demonstrated herein paves the way for the design of next-generation biofunctional materials with enhanced performance and stability. Moreover, this approach supports the principles of the circular economy through the valorization of agro-industrial by-products, while simultaneously contributing to the advancement of innovative medical, protective, and personal care textiles with significant societal and industrial impact.

2. Materials and Methods

2.1. Materials

The study utilized blackcurrant pomace sourced from Floriva (Ivanjica, Serbia), which was lyophilized, ground in a mill, and had a moisture content of 5.6%. Bleached cotton fabric was procured from Alkaloid AD (Berovo, North Macedonia). Fabric coating reagents included chitosan (molecular weight 190,000–310,000 g/mol; degree of deacetylation 75–85%) from Carbosynth Limited (Compton, Berkshire, UK) and GRINDSTED® pectin LC 810 from P.I.C. Co. DOOEL (Skopje, North Macedonia). All reagents used for polyphenol analysis were of analytical grade and purchased from Sigma-Aldrich (Schnelldorf, Germany). Anthocyanin reference standards, including cyanidin-3-O-glucoside, cyanidin-3-O-rutinoside, delphinidin-3-O-glucoside, and delphinidin-3-O-rutinoside, were obtained from Carl Roth (Karlsruhe, Germany). HPLC-grade methanol and water, as well as trifluoroacetic acid (TFA), were also supplied by Sigma-Aldrich (Schnelldorf, Germany). Gallic acid (≥98.0% purity) and quercetin (≥95% purity) were obtained from Merck (Darmstadt, Germany). Microbial cultivation media, including trypticase soy broth, nutrient broth, and agar, were purchased from the Institute of Virology, Vaccines, and Sera "Torlak" (Belgrade, Serbia).

2.2. Optimization of Extraction Conditions Based on Total Phenolic Content (TPC)

Extraction parameters were optimized using response surface methodology (RSM) based on a three-factor, three-level Box–Behnken experimental design. The investigated variables were extraction time (5–45 min), ethanol concentration (20–80%), and liquid-to-solid ratio (5–45 mL/g DW). A total of 17 experimental runs were generated by the design, including replicated central points. The levels of the independent variables, expressed as both coded and actual values, are presented in Section 3.1. To minimize potential systematic errors, all experiments were performed in a randomized order.

Total phenolic content (TPC) of the obtained extracts was used as the response variable for model development. The experimental data were fitted to a second-order polynomial model according to Equation (1):

$$Y = \beta_{k0} + \sum_{i=1}^{3} \beta_{ki} X_i + \sum_{i=1}^{3} \beta_{kii} X_i^2 + \sum_{i=1}^{2} \sum_{j=i+1}^{3} \beta_{kij} X_i X_j \quad (1)$$

where Y represents the predicted response (TPC), β_{k0} is the intercept, β_{ki}, β_{kii}, and β_{kij} correspond to linear, quadratic, and interaction regression coefficients, respectively, while X_i and X_j denote the independent variables (extraction time, ethanol concentration, and liquid-to-solid ratio).

Experimental design generation, regression analysis, and parameter optimization were performed using Design Expert software (Version 8, Stat-Ease Inc., Minneapolis, MN, USA), with statistical significance assessed by analysis of variance (ANOVA). The predictive capability of the model was further verified by performing an additional experiment (in triplicate) under the calculated optimal extraction conditions.

2.3. Chemical Characterization of the Extract

The total phenolic content of the obtained extracts was determined using a modified Folin–Ciocalteu assay. The results were expressed as milligrams of gallic acid equivalents per gram of dry weight of the pomace (mg GAE/g DW). Total flavonoid content (TFC) was evaluated using the aluminum chloride colorimetric method and reported as milligrams of quercetin equivalents per gram of dry weight (mg QE/g DW). Both analyses were performed following previously reported procedures [16].

Anthocyanin composition of the extract obtained under optimized extraction conditions was analyzed by reverse-phase high-performance liquid chromatography (RP-HPLC). Chromatographic separation was performed using a Dionex Ultimate 3000 HPLC system (Thermo Scientific, Waltham, MA, USA) equipped with a ZORBAX Eclipse Plus C18 reverse-phase column (4.6 mm × 150 mm, 5 µm). The separation protocol followed an established method for anthocyanin analysis [17]. Detection of anthocyanins, including cyanidin-3-O-glucoside, cyanidin-3-O-rutinoside, delphinidin-3-O-glucoside, and delphinidin-3-O-rutinoside, was conducted at 520 nm. Before chromatographic analysis, the extract was concentrated by removing solvent under reduced pressure using a Rotavapor R-210 rotary evaporator (Buchi, Flawil, Switzerland), reducing the volume to approximately one-tenth of the initial extract volume.

2.4. Fabric Functionalization with Bioactive Compounds

2.4.1. Preparation of Solutions for Layer-by-Layer (LbL) Functionalization of Cotton Fabric with Bioactive Compounds

A cationic chitosan (CH) solution (0.5 wt%) was prepared by dissolving the polysaccharide in deionized (DI) water acidified to pH 1.7 with concentrated HCl. The final pH was adjusted to 4.0 using NaOH. An anionic pectin (P) solution (0.5 wt%) was prepared by dissolving pectin in DI water, followed by homogenization and pH adjustment to 4.0 with HCl. Both solutions were stirred for 24 h.

For the functionalization process of cotton fabric with bioactive compounds, binary mixtures were prepared by combining equal parts of the polysaccharide solutions with a 2% blackcurrant pomace extract (BC). These mixtures, designated as CH-BC and P-BC, contained final concentrations of 0.25% polysaccharide and 1% extract. The pH of the CH-BC and P-BC mixtures was adjusted to pH 4.0 prior to the LbL deposition process. Control solutions of 0.25% CH and 0.25% P (without extract) were prepared following the same procedure used for the 0.5% CH and 0.5% P solutions, respectively.

2.4.2. LbL Functionalization of Cotton Fabric with Bioactive Compounds

The cotton fabric was biofunctionalized using a dip-coating LbL technique involving alternating immersion in two oppositely charged solutions, CH-BC and P-BC, interspersed with rinsing steps (Figure 2). The formation of bilayer (BL) involved a 5 min fabric immersion in the cationic solution, a deionized (DI) water rinse (for 1 min to remove excess solution and unbound compounds), a 5 min immersion in the anionic solution, and a deionized (DI) water rinse. For all subsequent BLs, the immersion time was reduced to 1 min per solution. To maintain consistent concentration and purity, both the polyelectrolyte solutions and the rinsing water were replaced after every fourth BL. After completion of the LbL functionalization, a final rinsing step was performed to ensure the removal of any residual solutions and loosely bound compounds. The LBL functionalization of cotton fabric was carried out in a shaking water bath at a temperature of 22 ± 1 °C, and then the coated fabrics were air-dried at room temperature. The labels for all functionalized samples are detailed in Table 1.

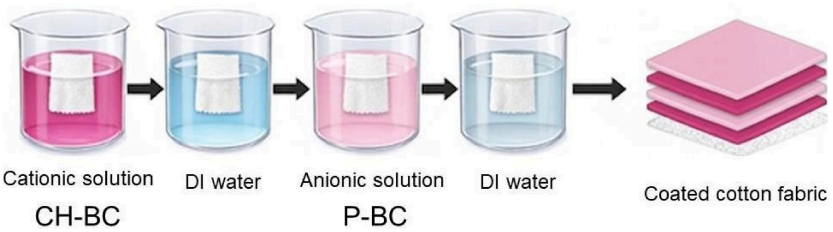


Figure 2. Process workflow for the LbL functionalization of cotton fabric with bioactive compounds.

Table 1. Cotton fabric labels and description of the functionalization treatments.

Sample	Explanation
CO	Non-functionalized cotton fabric
4BL CH/P	4BL of 0.25% CH and 0.25% P
8BL CH/P	8BL of 0.25% CH and 0.25% P
12BL CH/P	12BL of 0.25% CH and 0.25% P
COBC	Traditional functionalization with 2% BC
4BL CH-BC/P-BC	4BL of 0.25% CH-1% BC/0.25% P-1% BC
8BL CH-BC/P-BC	8BL of 0.25% CH-1% BC/0.25% P-1% BC
12BL CH-BC/P-BC	12BL of 0.25% CH-1% BC/0.25% P-1% BC

2.4.3. Traditional Functionalization of Cotton Fabric with Bioactive Compounds

For comparison, cotton fabric was biofunctionalized via a traditional exhaustion method using a 2% blackcurrant pomace extract solution at a fabric-to-liquid ratio of 1:30. The functionalization process was conducted in a Linitest apparatus for 30 min at 22 ± 1 °C. This specific duration was chosen to synchronize with the total processing time required for the deposition of 12BL of CH-BC/P-BC, thereby ensuring that the exposure time to the extract remained consistent across both functionalization techniques.

2.5. Protocols for Evaluating Fabric Biofunctional Properties

The antioxidant activity of the fabric was assessed using the ABTS assay according to the method reported by Pavun et al. [18]. Briefly, 0.1 g of each fabric was added to a test tube containing 3.9 mL of freshly prepared $ABTS^{\bullet+}$ radical cation solution, and the reaction took place in the dark at 25 °C for 30 min. The fabric radical scavenging activity was determined by measuring the absorbance of the solution at 734 nm, and the antioxidant activity was calculated according to Equation (2).

$$antioxidant\ activity\ (\%) = \frac{A_C - A_S}{A_C} \times 100 \quad (2)$$

where A_c is the absorbance of the control solution (containing the reagent except the fabric), while A_s is the absorbance of the control solution containing the fabric. Antioxidant experiments were performed in triplicate.

The antimicrobial activity of the studied fabrics was evaluated against the Gram-negative bacterium *E. coli* ATCC 25,922 and the Gram-positive bacterium *S. aureus* ATCC 25923, both obtained from American Type Culture Collection (Rockville, MD, USA). Before testing, the fabrics were sterilized in an autoclave at 121 °C for 15 min. Bacterial inocula were prepared by transferring a single colony of the test organism into the growth medium (nutrient broth for *E. coli* and tryptic soy broth for *S. aureus*) and incubating at 37 °C under shaking conditions. Briefly, 0.2 g of the tested fabric was placed in 9 mL of sterile saline solution and inoculated with 1 mL of bacterial suspension to obtain a final bacterial concentration of ~10^5 CFU/mL. After a contact period of 24 h at 37 °C with shaking, aliquots were collected, serially diluted, and spread onto agar plates. The plates were then incubated at 37 °C for 24 h, after which the resulting colonies were counted. The percentage of antibacterial activity was calculated according to Equation (3) [19]:

$$R\ (\%) = \frac{C_0 - C_t}{C_0} \times 100 \quad (3)$$

where C_0 represents the initial bacterial concentration (CFU/mL), and C_t denotes the bacterial concentration (CFU/mL) after 24 h of contact with the fabric. Antimicrobial

activity was evaluated in triplicate, and the obtained results exhibited a coefficient of variation of less than 1.34%.

The cytotoxicity of CO and LbL-functionalized fabrics (4BL CH-BC/P-BC, 8BL CH-BC/P-BC, and 12BL CH-BC/P-BC) was assessed using the MTT assay on cultured human keratinocyte cells (HaCaT cell line), following the protocol previously described in the literature [20]. All experiments were performed in triplicate, with the coefficient of variation maintained below 2.7%.

The determination of the pH of aqueous extract of fabrics was done according to the standard ISO 3071:2020 [21].

2.6. Coloration Properties of Biofunctionalized Cotton Fabrics

Fabric CIELab coordinates (L*, a*, and b*) were determined using an X-Rite Color i7 spectrophotometer (Kentwood, MI, USA). Measurements were performed under a D65 illuminant with a 10° standard observer. The L* value indicates the lightness of the fabric, where lower values correspond to more intensely colored fabrics. The a* coordinate represents chromaticity ranging from green (−a*) to red (+a*) axis, while the b* coordinate reflects chromaticity from blue (−b*) to yellow (+b*). The color strength (K/S) values of the fabrics were calculated from the reflectance values recorded using a UV–Vis spectrophotometer (Shimadzu UV-2600, Kyoto, Japan), according to the Kubelka–Munk equation.

2.7. Moisture Management Properties of Cotton Fabrics

The moisture management properties of the selected fabrics were evaluated and classified in accordance with AATCC TM 195-2017 [22] standard using a Moisture Management Tester M290 (MMT, SDL Atlas, Rock Hill, SC, USA). The results are presented as mean values accompanied by coefficients of variation for each measured parameter, including wetting time (WT) for the top (T) and bottom (B) surfaces, absorption rate (AR) for the top and bottom surfaces, maximum wetted radius (MWR) for the top and bottom surfaces, spreading speed (SS) for the top and bottom surfaces, accumulative one-way transport capability (R), and overall moisture management capability (OMMC). Based on the measured properties, the MMT M290 system classified the fabrics and generated their characteristic performance fingerprints.

2.8. Contact Angle of Cotton Fabrics

The contact angle was measured according to ISO 19403-6:2024 [23] standard by changing the volume of a drop using the Drop Shape Analyzer DSA30S goniometer (KRÜSS GmbH, Hamburg, Germany). Using the standard configuration of the DSA30S, the dynamic advancing contact angle with water was determined. A sample size of 4 cm × 4 cm and three different drop measurements are required by the standard. During each measurement, the DSA30S dispenses a 10 µL drop and takes at least 20 photos over 2 s. Afterwards, the DSA30S software determines the contact angle from each photo and calculates it. All tests were conducted in triplicate under controlled laboratory conditions (23 ± 2 °C and relative humidity of 50 ± 5%).

2.9. Molecular Docking Simulations

2.9.1. Preparation of Polymer Receptors

Three polysaccharide-based polymers, cellulose, chitosan, and pectin, were used as receptors in molecular docking simulations. Initial three-dimensional structures of the polysaccharide oligomers were constructed using the GLYCAM-Web Carbohydrate Builder [24], which enables accurate generation of carbohydrate structures with correct glycosidic linkages and stereochemistry. Linear oligomers consisting of ten monomeric units were generated for each polymer as simplified representative models of the polysaccharide

surfaces. This chain length was selected as a compromise between structural representativeness and computational feasibility; it provided a sufficiently extended polymer surface with multiple potential binding sites for the anthocyanin glycosides while avoiding the excessive molecular size and computational complexity associated with longer polymer chains. The same number of monomeric units was used for cellulose, chitosan, and pectin to enable a consistent comparison of their relative ligand-binding affinities. Linear oligomers consisting of ten monomeric units were generated for each polymer to represent the surface while maintaining computational feasibility.

Cellulose was modeled as a linear β-(1,4)-D-glucan oligomer, while pectin was represented by a homogalacturonan backbone composed of α-(1,4)-D-galacturonic acid units. Chitosan oligomers were generated from a chitin precursor consisting of β-(1,4)-linked N-acetyl-D-glucosamine units. The conversion of chitin into chitosan was performed in silico by manual structural editing in BIOVIA Discovery Studio (Dassault Systèmes, San Diego, CA, USA) [25]. Specifically, the acetyl moiety of each N-acetyl group was removed, converting the acetamide functionalities of the chitin precursor into primary amino groups and yielding β-(1,4)-linked glucosamine units characteristic of chitosan. This procedure generated a fully deacetylated decameric chitosan model, which was used as an idealized receptor structure for comparative molecular docking analysis, rather than as an exact representation of the heterogeneous degree of deacetylation of the experimental bulk polymer.

To simulate the acidic conditions of the experimental working solution (pH ~ 4), all amino groups in chitosan were treated as fully protonated ($–NH_3^+$), consistent with the pK_a of chitosan amino groups. Carboxyl groups of pectin were set in their deprotonated carboxylate form ($–COO^-$), while cellulose hydroxyl groups were kept in their neutral form. Following these adjustments, all polymer structures were subjected to geometry optimization and energy minimization via Avogadro (version 1.2.0) [26] using the Universal Force Field (UFF) and the steepest descent algorithm to remove unfavorable steric interactions. Prepared polymer receptors were further processed using AutoDockTools (ADT) [27] to add polar hydrogen atoms and assign Gasteiger partial atomic charges. Final receptor structures were saved in PDBQT format for subsequent docking simulations.

2.9.2. Ligand Preparation

Four anthocyanin glycosides: cyanidin-3-O-glucoside, cyanidin-3-O-rutinoside, delphinidin-3-O-glucoside, and delphinidin-3-O-rutinoside, were used as ligands for the docking study. The initial three-dimensional ligand structures were obtained from the PubChem database and subjected to geometry optimization using Avogadro (version 1.2.0) with the UFF force field. Further ligand preparation for docking was carried out using ADT, where polar hydrogen atoms were added, Gasteiger partial charges were assigned, and rotatable bonds were defined. Each ligand structure met the ADT torsional flexibility requirements before being exported in PDBQT format for the final simulations.

2.9.3. Docking Protocol

Molecular docking simulations were performed using AutoDock 4.2.6, employing the Lamarckian Genetic Algorithm (LGA). For each polymer receptor, a grid box was defined to encompass the entire oligomeric structure, allowing ligand exploration across the polymer surface. The grid spacing was set to 0.375 Å, with grid dimensions individually adjusted to fully cover each polymer oligomer. Grid maps were generated using AutoGrid4, and docking simulations were conducted with 200 genetic algorithm runs per ligand–receptor pair. All other docking parameters were kept at default values. Docking results were analyzed using ADT, and the most favorable binding poses were manually selected based

on the lowest binding energy within the most populated clusters. Representative docking poses and the resulting intermolecular interactions were visualized and analyzed using BIOVIA Discovery Studio.

3. Results and Discussion

3.1. Optimization of Extraction Conditions and Extract Characterization

The extraction conditions were statistically optimized using a designed experimental plan based on the Box–Behnken design. This approach enabled a systematic evaluation of both the individual and interactive effects of the selected extraction variables, while simultaneously reducing the number of required experimental runs. The results obtained for each experimental combination, along with the corresponding experimental conditions under which they were obtained, are presented in Table 2.

Table 2. Experimental design and corresponding results for total phenolic content (TPC).

Run	Time, Min	Ethanol Concentration, %	Liquid-to-Solid Ratio, mL/g DW	TPC, mg GAE/g DW
1	45	80	25	22.43
2	25	20	45	21.36
3	25	50	25	33.52
4	25	80	45	23.65
5	**25**	**50**	**25**	**35.24**
6	5	50	5	14.13
7	45	50	45	33.52
8	5	80	25	16.00
9	45	20	25	31.24
10	25	50	25	32.88
11	5	50	45	19.24
12	25	50	25	33.05
13	25	50	25	32.89
14	25	20	5	14.50
15	**25**	**80**	**5**	**11.04**
16	5	20	25	14.16
17	45	50	5	16.84

As shown in Table 2, a pronounced variability in TPC values was observed across the experimental runs, indicating that, within the examined parameter ranges, the extraction conditions had a substantial influence on phenolic yield. The highest TPC was obtained in run 5 (35.24 mg GAE/g DW), where all three process parameters were set at their central levels. In contrast, the lowest TPC yield was observed in run 15 (11.04 mg GAE/g DW), conducted at the mid-level extraction time, the highest ethanol concentration, and the lowest liquid-to-solid ratio. The experimental data were further evaluated using one-way ANOVA, and the corresponding statistical results are presented in Tables S1 and S2, Supplementary Material. The model F-value of 29.60 indicates that the model is statistically significant, with only a 0.01% probability that such a high F-value could arise from random noise. Model terms with *p*-values lower than 0.0500 were considered statistically significant; in this case, the linear effects of time (A) and liquid-to-solid ratio (C), their interaction terms (AB and AC), as well as three quadratic terms, had a significant impact on the response (Table S1, Supplementary Material). To comply with model hierarchy, the linear term corresponding to ethanol concentration (B) was retained in the final model despite its lack of statistical significance (*p*-value of 0.2124). The lack-of-fit F-value of 1.05 suggests that lack of fit is not significant relative to the pure error, confirming that the proposed model adequately describes the experimental data. Furthermore, the predicted R^2 (0.8237)

is in reasonable agreement with the adjusted R^2 (0.9346), as the difference is less than 0.2 (Table S2, Supplementary Material). The adequate precision value of 14.6261 indicates an adequate signal-to-noise ratio, demonstrating that the model is suitable for navigating the design space.

The final quadratic model, expressed in terms of coded variables, is presented by Equation (4):

$$TPC = 32.32 + 5.06A - 1.02B + 5.16C - 2.66AB + 2.89AC - 4.03A^2 - 7.33B^2 - 7.35C^2 \quad (4)$$

The influence of all three parameters was described by linear terms (positive for extraction time and liquid-to-solid ratio and negative for ethanol concentration) as well as by negative quadratic terms, which means that their influence was described by quadratic functions with maxima within the examined ranges. The model also included a statistically significant negative interaction between extraction time and ethanol concentration, as well as a positive interaction between time and liquid-to-solid ratio. The negative interaction between time and ethanol concentration suggests that, at lower ethanol concentrations, longer extraction times may be required to achieve complete extraction. Conversely, at higher ethanol concentrations, extended times can lead to polyphenol degradation and a decrease in yield. Such an inverse relationship has been previously reported, highlighting the importance of statistical optimization of extraction parameters that takes into account interactions between parameters [28]. Furthermore, the positive interaction observed between time and liquid-to-solid ratio implies that the simultaneous increase in both factors within the examined ranges enhances the extraction yield. This relationship is driven by mass transfer principles: a higher liquid-to-solid ratio increases the solvent's capacity for dissolving polyphenols, while longer extraction times facilitate their transfer from the solid matrix into the solvent, up to the point of equilibrium [29]. The shifts in local maxima caused by these interactions are illustrated in Figure 3.

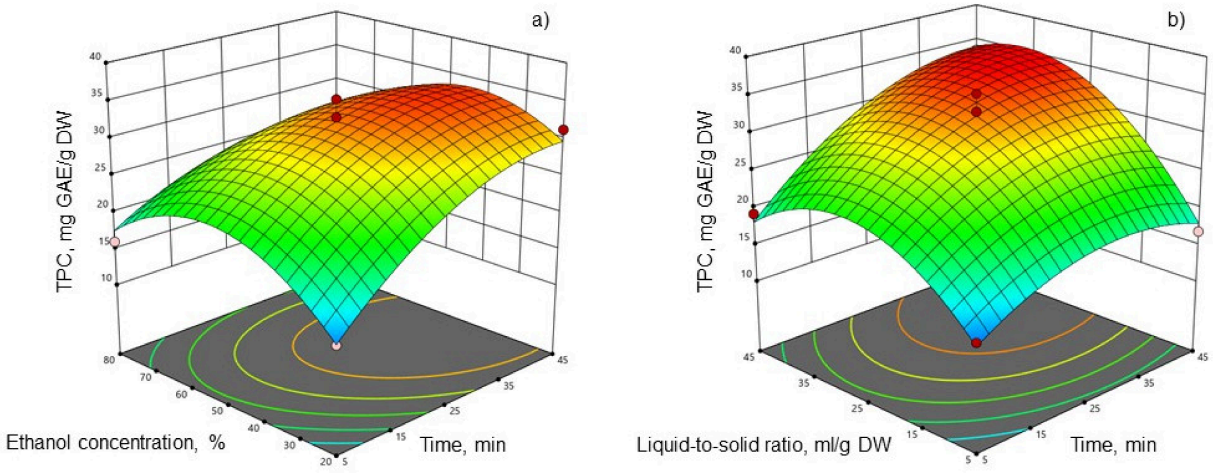


Figure 3. Response surface plots illustrating the interactive effects of: (**a**) extraction time and ethanol concentration at a fixed liquid-to-solid ratio of 25 and (**b**) extraction time and liquid-to-solid ratio at a fixed ethanol concentration of 50%.

To determine the optimal extraction conditions that maximize the TPC yield, numerical optimization was performed in Stat Ease Design Expert. The optimization yielded the following conditions: 42.9 min, 43.0% ethanol and 35.5 mL extraction medium per gram of dry blackcurrant pomace. Under these conditions, the model predicted a TPC yield of 36.05 mg GAE/g DW. To validate the model and optimization results, an additional experiment was conducted under the predicted optimal conditions. The experimentally

obtained TPC was 36.04 ± 0.25 mg GAE/g DW, corresponding to a deviation of only 0.028% from the predicted value. This negligible difference indicates excellent agreement between the predicted and experimental results, thereby confirming the accuracy of the model and the reliability of the optimization procedure.

It should be noted that a comparable TPC value was also obtained at the central design point under different extraction conditions, i.e., a lower liquid-to-solid ratio and a shorter extraction time but a higher ethanol concentration. These findings suggest that multiple combinations of extraction parameters yield similarly high TPC. Such flexibility indicates that alternative operating conditions may be selected based on specific process priorities, such as minimizing solvent consumption or enhancing space–time yield, while still maintaining high phenolic recovery from blackcurrant pomace. Nevertheless, the statistically optimized conditions resulted in the highest predicted and experimentally confirmed responses, thus justifying their selection as the optimal extraction parameters. Under these conditions, the TFC of the blackcurrant pomace extract, quantified using the aluminum chloride colorimetric method, reached 5.28 mg ± 0.12 QE/g DW.

Additional characterization of the extract obtained under optimized conditions was performed by quantifying individual anthocyanins. Blackcurrant anthocyanins contribute not only to the extract's high antioxidant capacity but also act as natural colorants. Reverse-phase HPLC analysis (Figure S1, Supplementary Material) identified four dominant anthocyanins, and their retention times and concentrations are summarized in Table 3. The extraction process yielded particularly high quantities of delphinidin-3-O-rutinoside (Del3Rut, 2.384 mg/g DW) and cyanidin-3-O-rutinoside (Cya3Rut, 1.998 mg/g DW), alongside lower amounts of the corresponding glucosides, delphinidin-3-O-glucoside (Del3Glu, 0.556 mg/g DW) and cyanidin-3-O-glucoside (Cya3Glu, 0.242 mg/g DW). This composition is characteristic of blackcurrant matrices, in which rutinosides of cyanidin and delphinidin generally dominate the total anthocyanin content, whereas their glucosides occur in minor proportions, largely independent of the extraction method. Such a profile is widely reported across cultivars, processing conditions, and extraction solvents, demonstrating the robustness of anthocyanin composition in *Ribes nigrum* materials [17,30,31]. All identified anthocyanins are recognized for their strong antioxidant activity and exhibit intense, pH-dependent coloration over a broad pH range. Moreover, the predominance of rutinoside anthocyanins, which are associated with enhanced color stability relative to glucosides, further underscores the suitability of blackcurrant extracts for one-step textile functionalization and dyeing [30].

Table 3. Anthocyanin composition of the blackcurrant pomace extract obtained under optimized conditions (λ—wavelength, Rt—retention time).

Compound	Retention Time, Min	Concentration, mg/g DW
delphinidin-3-O-glucoside	26.050	0.556 ± 0.016
delphinidin-3-O-rutinoside	27.173	2.384 ± 0.022
cyanidin-3-O-glucoside	28.557	0.242 ± 0.014
cyanidin-3-O-rutinoside	29.560	1.998 ± 0.034

3.2. Cotton Fabrics' Biofunctional Properties

To develop biofunctional and skin-comfortable polysaccharide-based textiles with potential healthcare applications, an optimized blackcurrant pomace extract was incorporated into a chitosan/pectin LbL coating. Specifically, the cotton fabrics were biofunctionalized with four, eight, or twelve BLs of the extract-enriched polyelectrolytes, denoted as 4BL CH-BC/P-BC, 8BL CH-BC/P-BC, and 12BL CH-BC/P-BC, respectively. Additional cotton fabrics were prepared to assess the individual effects of the extract and LbL coating protocol

on fabric biofunctional properties. These included non-functionalized cotton (CO), cotton coated with 4, 8, or 12 BLs of chitosan/pectin without the blackcurrant pomace extract (4BL CH/P, 8BL CH/P, and 12BL CH/P, respectively), and cotton biofunctionalized solely with the extract via a conventional exhaustion method (COBC). After air-drying at room temperature, all eight fabrics were evaluated for their biofunctional properties, including antioxidant and antibacterial activities.

3.2.1. Fabric Antioxidant Activity

The non-functionalized cotton fabric (CO) exhibited an antioxidant activity of 21.11% (Figure 4), which can be attributed to the cellulose structure and the oxidation of functional groups during the bleaching process, both of which enable limited radical-scavenging interactions. This result is in good agreement with the findings reported by Freitas et al. [3], who likewise observed low antioxidant activity (27.4%) of untreated cotton. Functionalization of cotton fabric with various numbers of chitosan/pectin BLs results in a moderate increase in antioxidant activity, reaching values in the range of 36.03–39.04%. The observed enhancement in antioxidant activity of 4BL CH/P, 8BL CH/P, and 12BL CH/P fabrics, compared with the CO fabric, can be explained by the increasing deposition of polysaccharides on the fabric surface (2.16, 3.30, and 4.03% calculated weight gains, respectively; Figure 4), which enhances the availability of functional groups capable of participating in redox interactions. In theory, the hydroxyl and amino groups (–OH and $–NH_2$) present in chitosan macromolecules may contribute to radical-scavenging interactions through hydrogen donation and metal-chelating mechanisms [32]. Nevertheless, several studies have reported that native chitosan exhibits low or even negligible antioxidant activity [33,34]. Moreover, Wang et al. [35] observed that a 0.25% pectin solution (as used in the current study, Section 2.4.1) showed limited radical-scavenging capacity (<15%). The relatively modest enhancement suggests that the polysaccharide-based coatings alone provide only limited antioxidant functionality of fabrics in the absence of additional bioactive compounds.

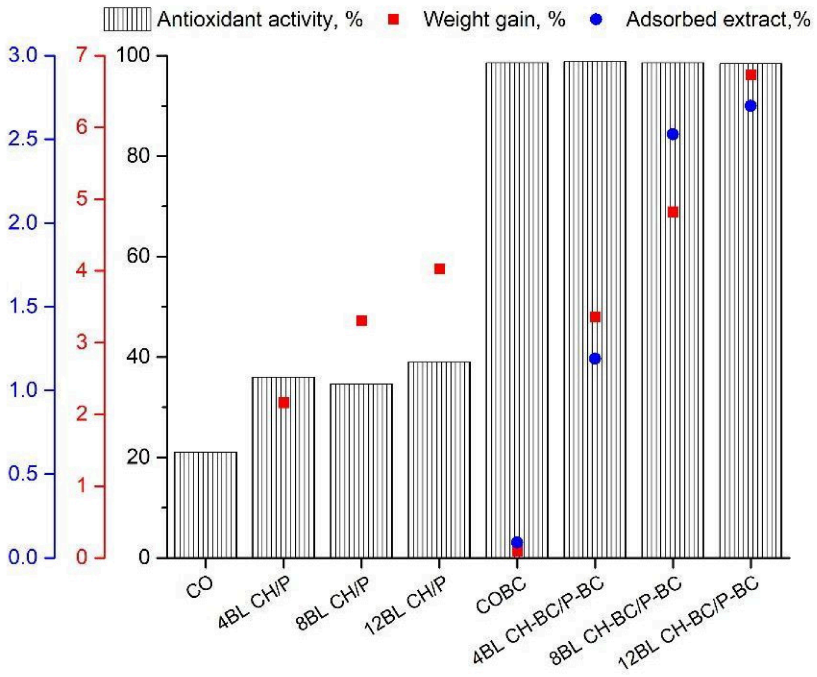


Figure 4. Fabrics' antioxidant activity, weight gain, and percentage of adsorbed blackcurrant pomace extract.

A pronounced fabric antioxidant activity is observed when blackcurrant pomace extract is used for cotton functionalization. Namely, the conventionally biofunctionalized COBC fabric demonstrates a significant increase in antioxidant performance, reaching nearly complete activity (98.57%) (Figure 4). This elevated antioxidant capacity can be ascribed to the adsorbed extract, particularly to its anthocyanins (Table 3), which represent a key class of polyphenolic compounds known for their beneficial role in maintaining overall health and supporting antioxidant defense systems [36,37]. Furthermore, fabrics biofunctionalized via the LbL approach with extract-enriched polyelectrolytes (4BL CH-BC/P-BC, 8BL CH-BC/P-BC, and 12BL CH-BC/P-BC) maintain similarly high antioxidant activity as COBC, indicating that the lowest number of BLs is sufficient to achieve full functionalization when the extract is effectively immobilized within the coating structure. These findings highlight the dominant role of extract-derived phenolic compounds as highly effective radical scavengers, while the number of deposited BLs mainly influences the percentage of adsorbed extract rather than the antioxidant capacity (Figure 4).

3.2.2. Antibacterial Activity of Fabrics

Building upon the demonstrated antioxidant performance, the effectiveness of functionalization strategies was further evaluated in terms of antibacterial activity of cotton fabrics. It was assessed against two pathogenic bacteria, *S. aureus* and *E. coli*, which are commonly associated with severe skin infections and wound complications [38]. It should be emphasized that the inhibition of *S. aureus* is of particular clinical importance, as its overgrowth is closely associated with the exacerbation of atopic dermatitis and the deterioration of existing skin lesions [39]. The experimental data presented in Figure 5 revealed that the CO fabric did not exhibit antibacterial activity against both tested bacteria. This behavior is expected, as the hydrophilicity and moisture retention capacity of cotton do not confer antibacterial properties; on the contrary, they may facilitate the adhesion, colonization, and proliferation of microorganisms, including *E. coli* and *S. aureus* [40]. However, cotton fabrics biofunctionalized with different numbers of chitosan/pectin BLs showed a progressive increase in antibacterial efficiency with increasing number of deposited BLs. While 4BL CH/P fabric did not inhibit bacterial growth, the 8BL CH/P fabric exhibited weak activity (24.47%) against *S. aureus* and almost complete inhibition (99.99%) of *E. coli* (Figure 5). The increased resistance of *S. aureus* compared to *E. coli* in 4BL CH/P fabric is most likely associated with the structural differences in bacterial cell walls [41]. Further increase in the number of BLs to 12 resulted in a substantial improvement in fabric antibacterial activity, particularly against *S. aureus*. This trend is driven by the increasing percentage of weight gain (Figure 4) and the formation of a thicker polyelectrolyte coating, which acts as a physical barrier that limits nutrient diffusion and bacterial adhesion. Moreover, the beneficial effects of chitosan and chitosan/pectin coatings on the antimicrobial activity of cotton have been previously reported in the literature [6,11].

The cotton fabric biofunctionalized only with blackcurrant pomace extract (COBC) did not show antibacterial activity, indicating that simple extract exhaustion and low adsorption (0.092%, Figure 4) are insufficient to ensure effective retention and sustained bioavailability of phenolic compounds. However, when blackcurrant pomace extract was incorporated into the LbL coating, a remarkable enhancement in fabric antibacterial efficiency was observed, even at the lowest number of BLs (Figure 5). Specifically, fabric 4BL CH-BC/P-BC demonstrated a 99.99% reduction in *E. coli* and an 87.87% reduction in *S. aureus*. With an increasing number of BLs (8BL CH-BC/P-BC and 12BL CH-BC/P-BC fabrics), antibacterial activity further improved, reaching nearly complete bacterial reduction. These results suggest that the LbL fabric coating effectively stabilizes the extract's polyphenolic compounds, ensuring a high concentration of antibacterial agents at the fabric

surface [10]. This statement was further supported by the linear correlations observed between the antibacterial activity of the fabrics 4BL CH-BC/P-BC, 8BL CH-BC/P-BC, and 12BL CH-BC/P-BC against *S. aureus* and the experimentally determined weight gain (r = 0.933) and the adsorbed blackcurrant pomace extract (r = 0.992). Observed antibacterial activity may be explained by mechanisms commonly reported for chitosan–polyphenol systems, including electrostatic interactions with bacterial cell envelopes and oxidative stress induced by phenolic compounds [41,42].

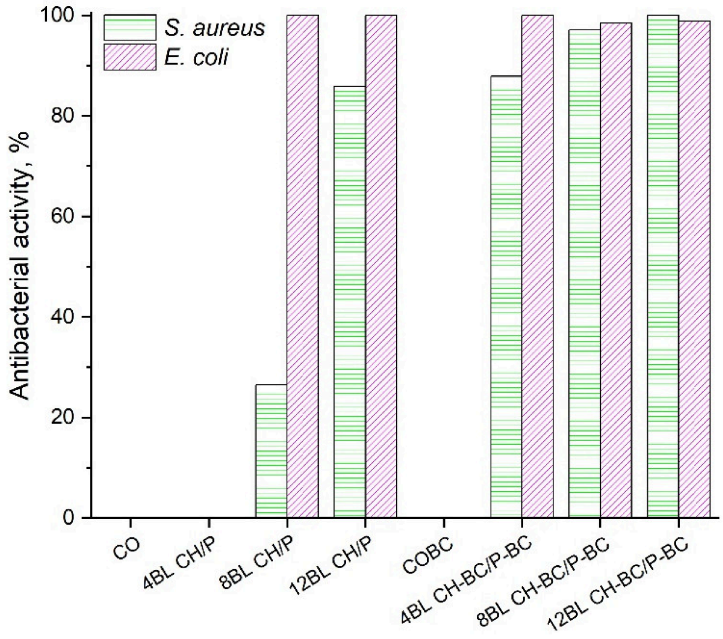


Figure 5. Fabrics' antibacterial activity.

3.2.3. Fabric Cytotoxicity

The cytotoxicity assessment of CO and LbL-functionalized fabrics (4BL CH-BC/P-BC, 8BL CH-BC/P-BC, and 12BL CH-BC/P-BC) was performed using human keratinocyte cells (HaCaT) in order to evaluate their suitability for skin-contact applications. As shown in Figure 6, all tested fabric extracts exhibited high cell viability values, ranging from 82.11% to 129.32%, regardless of extract concentration (100%, 50%, 25%, and 12.5%) and the number of deposited BLs. The CO fabric showed cell viability values above 80% for all tested extract concentrations, confirming that the cotton fabric itself did not exert cytotoxic effects on keratinocyte cells. After functionalization with bioactive compounds, the fabrics maintained or even improved cell viability compared to CO, indicating that the incorporation of chitosan, pectin, and blackcurrant pomace extract did not induce adverse cellular responses. In particular, the 8BL CH-BC/P-BC and 12BL CH-BC/P-BC fabrics demonstrated cell viability values exceeding 120% (Figure 6), suggesting not only good biocompatibility but also a possible stimulatory effect on keratinocyte metabolic activity. This behavior may be attributed to the presence of bioactive phenolic compounds originating from blackcurrant pomace extract, as well as the known biocompatibility of chitosan. According to ISO 10993-5 standard [43], materials are considered non-cytotoxic when cell viability remains above 80%. Therefore, all investigated fabrics can be classified as non-cytotoxic. The obtained results, together with the pH values of the fabric aqueous extracts (4.49, 4.44, and 4.44 for 4BLCH-BC/P-BC, 8BLCH-BC/P-BC, and 12BLCH-BC/P-BC, respectively), confirm that the developed bioactive fabrics exhibit excellent biocompatibility, which is particularly important for their potential skin-contact applications.

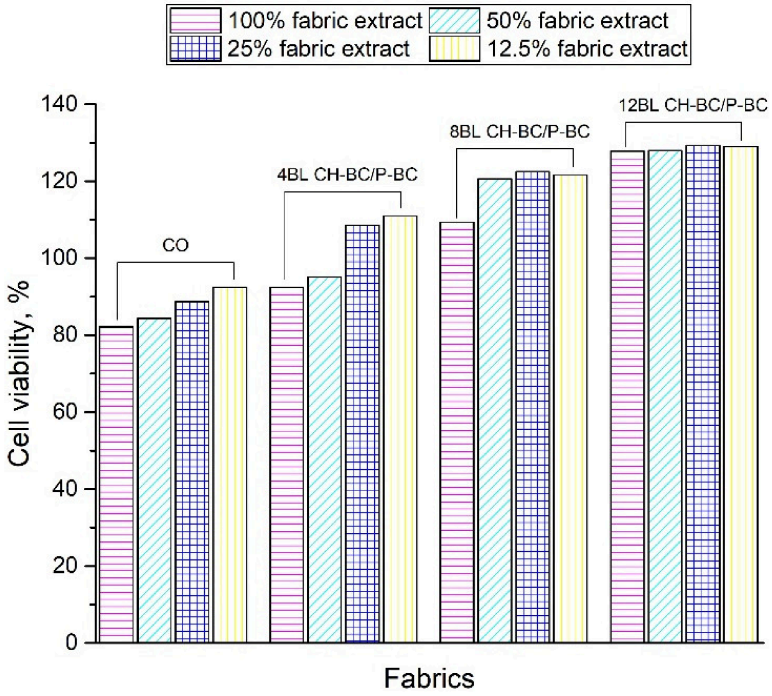


Figure 6. Cytotoxicity effect of fabrics' extracts on a HaCaT cell line.

The results presented in this section confirm that combining polyelectrolyte LbL deposition with bioactive extract incorporation is an effective strategy for developing biofunctional and biocompatible cotton fabrics, where the number of chitosan/pectin BLs represents a key parameter governing extract adsorption and, therefore, fabric biofunctional performance. Although the antioxidant and antibacterial activity of blackcurrant ethanol extracts has been extensively investigated in recent years [44–49], there is no information on the antioxidant, antibacterial, and cytotoxic performance of such extracts applied to cotton, either in unmodified form or upon modification/functionalization, which represents a limiting factor that precludes direct comparison of the results of the present study with previously published data.

3.3. Coloration Properties of Cotton Fabrics

The functionalization of cotton fabrics with bioactive compounds led to distinct changes in their visual appearance and coloration properties, which depend on the applied functionalization protocol and extract anthocyanins responsible for the wonderful colors of plant fruits [50]. As shown in Table 4, the traditionally biofunctionalized cotton (COBC) fabric displayed the highest lightness value (L* = 86.85), indicating only a slight coloration consistent with its very low percentage of adsorbed extract (0.09%, Figure 4). As the number of BLs in the LbL assembly increased from 4 to 12, the weight gain rose from 3.36% to 6.73%, while the percentage of adsorbed extract more than doubled from 1.19% to 2.70%. This adsorption of the blackcurrant extract is reflected in the CIELab coordinates, where the lightness (L*) decreased from 82.35 for 4BL CH-BC/P-BC to 78.38 for 12BL CH-BC/P-BC, indicating a darker fabric as more extract was incorporated into the polysaccharide-based matrix.

Simultaneously, the positive shift in a* values (from 2.91 to 4.02) and the pronounced increase in b* values (from 2.75 to 11.34) with increasing the percentage of adsorbed extract suggest the more intense reddish-yellow hues characteristic of anthocyanin-rich blackcurrant pomace extract. The particularly strong increase in yellowness (b* coordinate) from 2.75 to 11.34 demonstrated the enhanced optical contribution of LbL coatings, likely

arising from both increased extract adsorption and changes in light scattering associated with thicker polyelectrolyte assemblies. A similar trend was observed for the fabric color strength (K/S) values, which increased progressively from 0.08 for COBC to 0.15, 0.21, and 0.24 for 4BL CH-BC/P-BC, 8BL CH-BC/P-BC, and 12BL CH-BC/P-BC, respectively, indicating a gradual enhancement in color depth with increasing number of deposited BLs. The increase in K/S values confirms that the multilayer assemblies promoted greater retention of anthocyanins within the coating structure, resulting in more intense coloration of the cotton fabric. These findings demonstrate that the color coordinates and color strength of the biofunctionalized cotton fabrics are strongly governed by the combined effects of the LbL functionalization protocol, namely, weight gain, and the percentage of adsorbed extract, confirming that multilayer deposition represents an efficient strategy for improving both biofunctional properties and color intensity. According to the available literature, only one study has reported the use of blackcurrant as a natural colorant for cotton; specifically, Yasukawa et al. [51] employed fresh fruit as a dye source. In contrast, the present study proposes the valorization of blackcurrant pomace through the recovery and utilization of its bioactive colored compounds.

Table 4. Visual presentation, color coordinates (L*, a*, and b*), and color strength (K/S) values of the biofunctionalized cotton fabrics.

	Fabrics			
	COBC	**4BL CH-BC/P-BC**	**8BL CH-BC/P-BC**	**12BL CH-BC/P-BC**
Fabric Appearance				
Coloration Properties				
L*	86.85	82.35	79.72	78.38
a*	2.91	3.67	4.10	4.02
b*	2.75	6.85	9.52	11.34
K/S	0.08	0.15	0.21	0.24

3.4. Liquid Moisture Management Properties and Wetting of Selected Fabrics

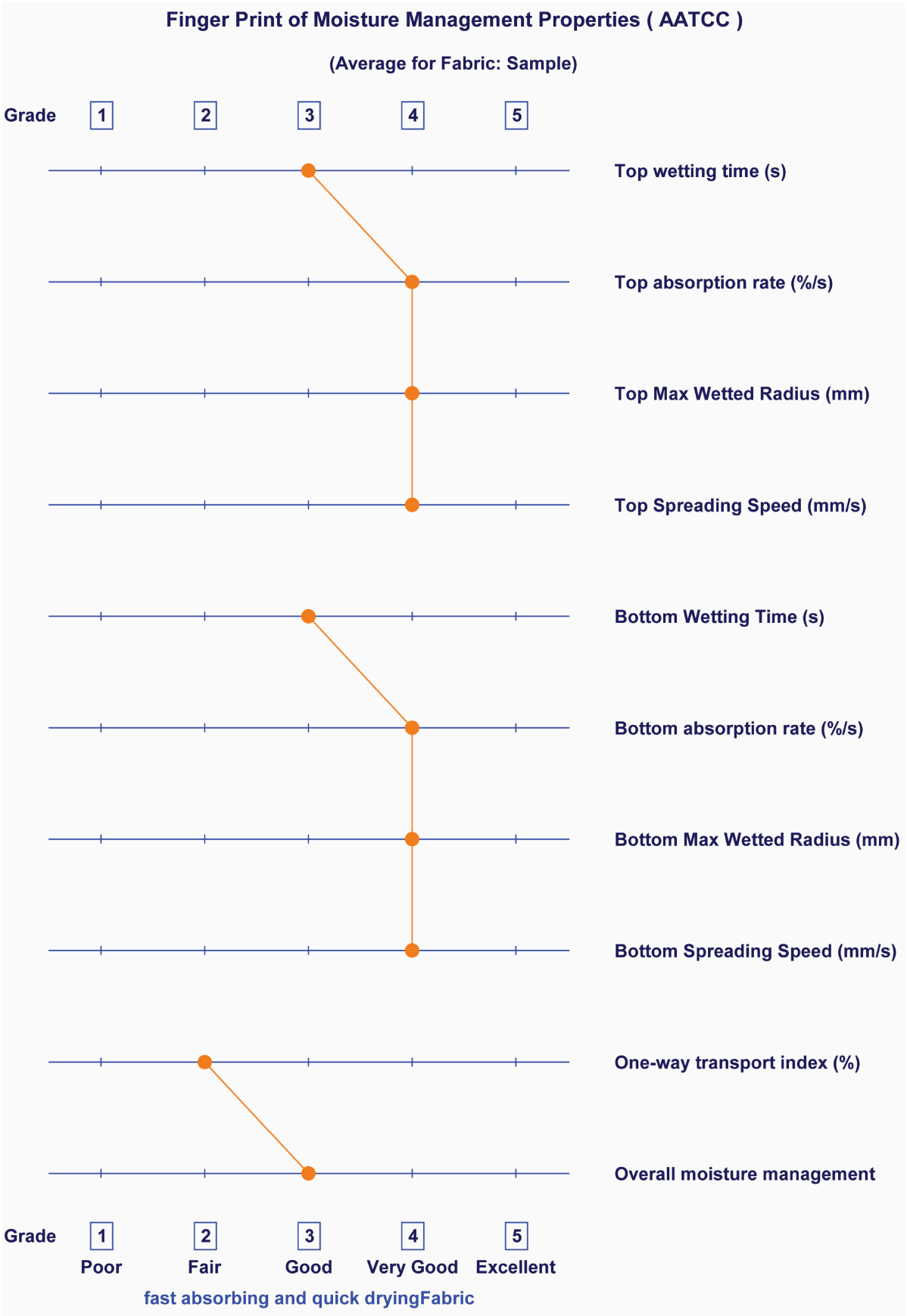
Given that liquid moisture management is recognized as one of the key performance parameters governing the thermo-physiological comfort of textile materials [52], this study evaluated the dynamic liquid moisture management properties of fabrics (Table 5) using a Moisture Management Tester (MMT) M290. According to the standardized test method in AATCC TM 195-2017 [22], the obtained results describe fabric wetting, its water repellency, penetration, absorption, or transport through the fabric, as well as the dynamic redistribution of liquid within and across the fabric thickness. To enable comparative interpretation of the liquid moisture management properties, the results are additionally presented in the form of fingerprints (Figure 7). In parallel, the contact angle of the fabrics was determined using a goniometer and is also presented in Table 5. Within this section, only the CO, 8BL CH/P, and 8BL CH-BC/P-BC fabrics were analyzed in order to elucidate the effect of the applied polysaccharide-based coatings and the extract incorporation on their comfort-related properties.

Table 5. The liquid moisture management properties and contact angle of selected fabrics.

Property	CO	8BL CH/P	8BL CH-BC/P-BC
Top wetting time, s	6.95 ± 1.25	10.41 ± 2.12	3.47 ± 0.19
Bottom wetting time, s	7.20 ± 1.05	10.64 ± 0.46	3.69 ± 0.30
Top absorption rate, %/s	74.61 ± 13.87	6.86 ± 0.12	23.07 ± 3.45
Bottom absorption rate, %/s	85.43 ± 3.93	18.93 ± 0.15	33.59 ± 1.98
Top maximum wetted radius, mm	20 ± 0	10 ± 0	20 ± 0
Bottom maximum wetted radius, mm	20 ± 0	10 ± 0	20 ± 0
Top spreading speed, mm/s	3.14 ± 0.22	0.64 ± 0.08	2.65 ± 0.13
Bottom spreading speed, mm/s	3.14 ± 0.13	0.60 ± 0.03	2.53 ± 0.22
Accumulative one-way transport capability, %	−0.80 ± 24.82	475.45 ± 23.02	120.14 ± 22.18
Overall (liquid) moisture management capacity	0.44 ± 0.03	0.52 ± 0	0.38 ± 0.01
Contact angle, CA°	64.71 ± 27.08	91.38 ± 7.66	52.86 ± 18.56

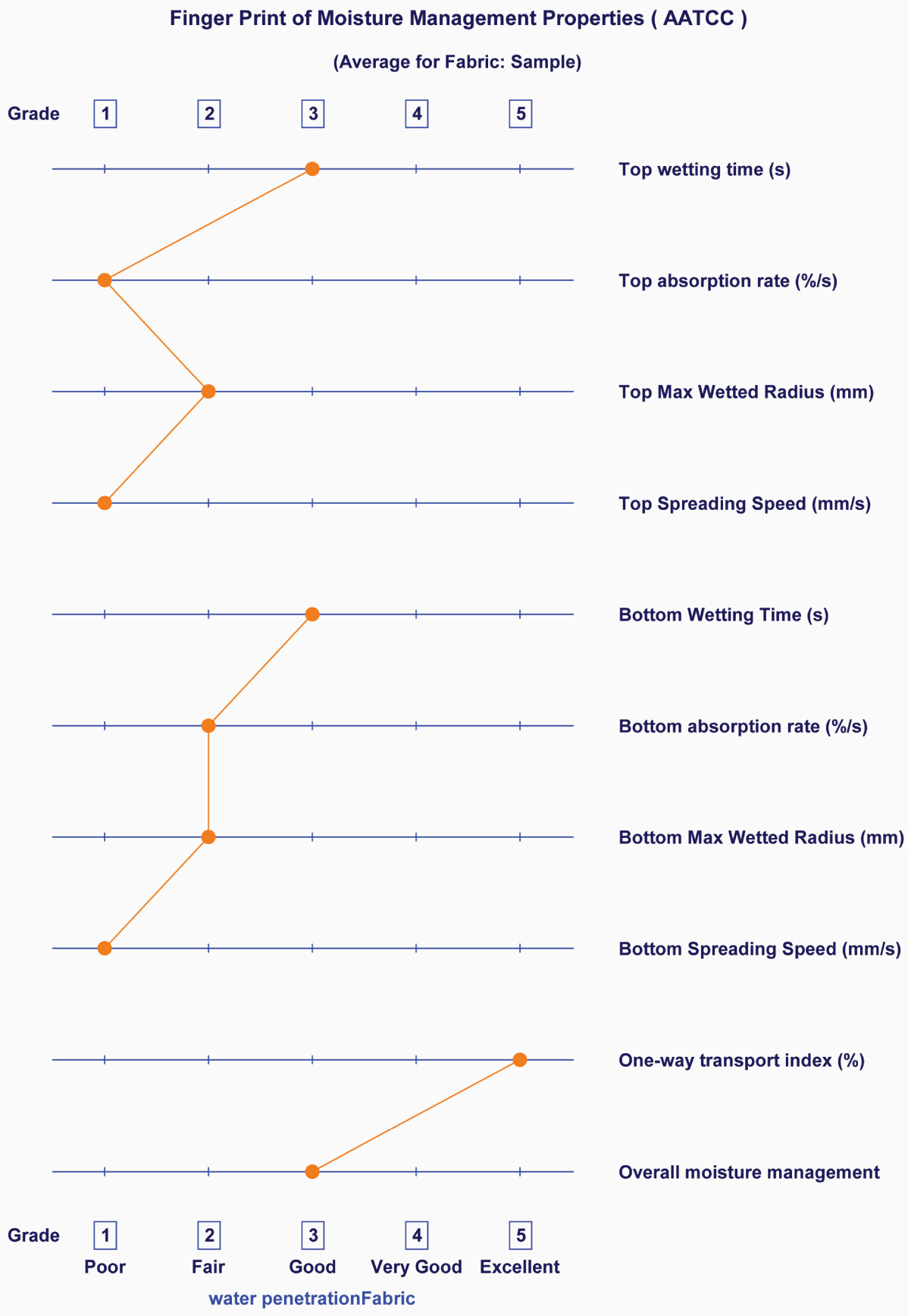
The CO fabric exhibited relatively moderate wetting times (~7 s) on both the top and bottom surfaces, high absorption rates, and maximum wetted radii of 20 mm, indicating a large spreading area and fast spreading (Table 5). The contact angle results further confirm its hydrophilic nature, as evidenced by the low contact angle of the CO fabric (64.71°), which is consistent with the observed moderate wetting time. Such behavior is typical for hydrophilic bleached cotton due to the abundance of accessible hydroxyl groups and the open capillary structure of the yarns, which facilitate fast liquid penetration and wicking. The near-zero and slightly negative one-way transport capability (−0.8%) suggests that the moisture does not preferentially move to one side but remains saturated throughout the structure. In other words, although CO readily absorbs moisture, it does not promote moisture pumping from the skin side to the outer surface. Consequently, the CO fabric demonstrated moderate overall moisture management capacity (0.44). According to the sample fingerprint (Figure 7a) and literature [53–55], CO is classified as a fast-absorbing and quick-drying fabric.

According to the same classification criteria and the sample fingerprint (Figure 7b), the cotton fabric coated with 8BLs of chitosan/pectin (8BL CH/P) is categorized as a water-penetration material. This behavior is evidenced by the small liquid spreading area (~0.6 mm/s) in combination with an exceptionally high one-way transport index (~475%) (Table 5). Compared with CO, the 8BL CH/P fabric exhibited prolonged wetting times and lower absorption rates, indicating increased resistance to initial liquid uptake, which can be ascribed to the formation of interpolymer electrostatic complexes between positively charged chitosan and negatively charged pectin, which likely created a dense, cohesive surface film that reduced surface energy heterogeneity and physically obstructed liquid diffusion pathways. This is further supported by contact angle measurements, as the 8BL CH/P fabric exhibited a higher contact angle (91.38°) compared to CO, confirming successful polysaccharide deposition and increased surface hydrophobicity. This increase in contact angle can be attributed not only to partial surface coverage but also to the restructuring of the textile surface and reduced pore accessibility [55]. Consequently, although the coated fabric shows strong resistance to surface wetting and spreading, once the liquid penetrates the surface barrier, it is efficiently transported toward the bottom side of the fabric. Therefore, the 8BL CH/P sample demonstrates a characteristic water-penetration mechanism coupled with highly directional moisture transfer. It should be pointed out that this fabric is not waterproof in the sense of preventing liquid water penetration; rather, it is a breathable fabric that allows the diffusion of water vapor (perspiration) through its structure.



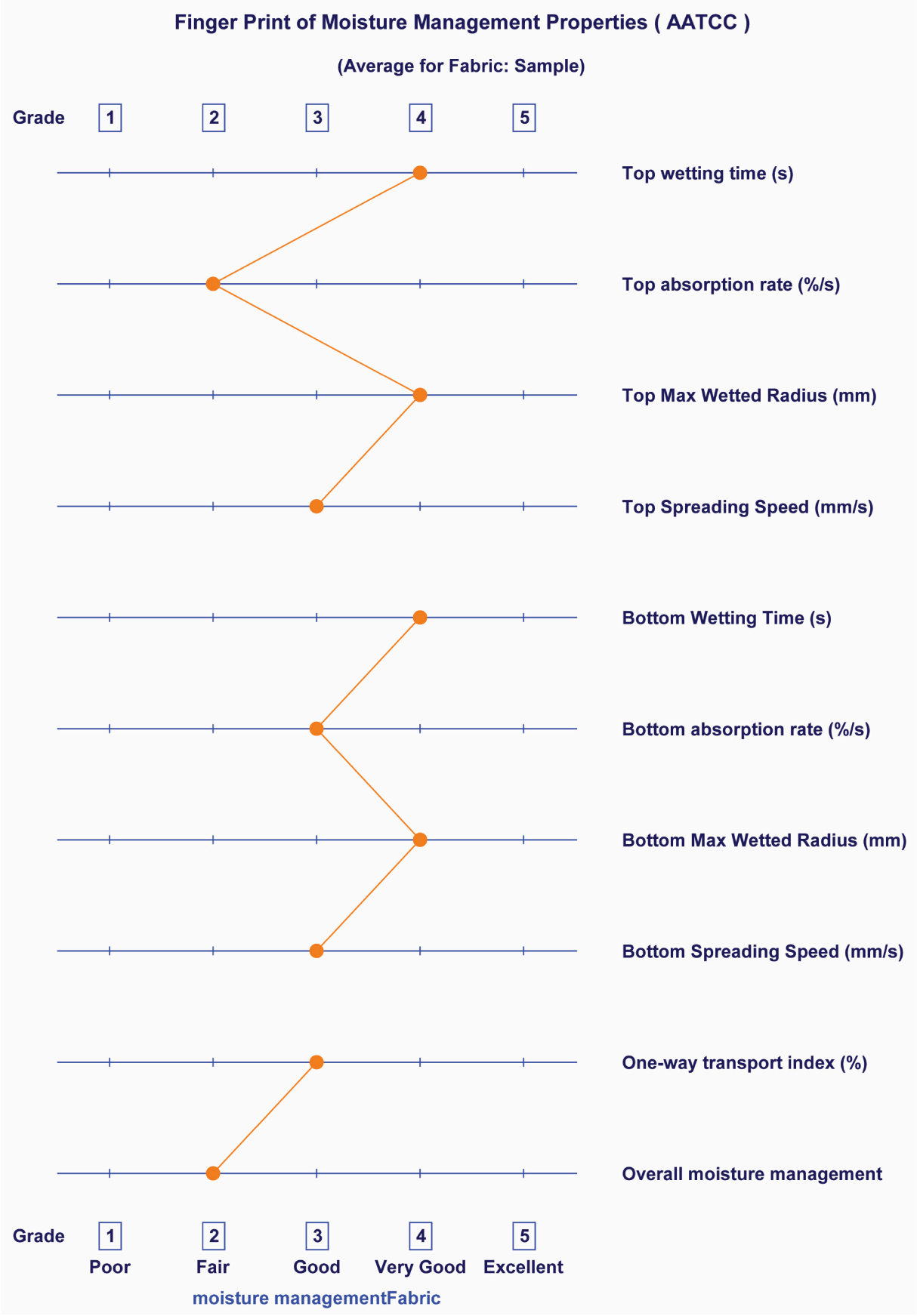
(**a**)

Figure 7. *Cont.*



(**b**)

Figure 7. *Cont.*



(**c**)

Figure 7. Fingerprint of moisture management properties of: (**a**) CO, (**b**) 8BL CH/P, and (**c**) 8BL CH-BC/P-BC.

The incorporation of blackcurrant pomace extract within the chitosan/pectin multilayer substantially altered the liquid transport performance of fabric 8BL CH-BC/P-BC. This modification also enhanced surface wettability, as reflected by the decrease in contact angle to 52.86° compared to that of 8BL CH/P (Table 5). However, the relatively high standard deviation value of 18.56° suggests rapid water absorption and non-uniform droplet spreading, which complicates precise contact angle determination. Furthermore, among the three tested fabrics, this fabric showed the shortest wetting times (~3.5 s) on both the top and bottom surfaces, increased absorption rates compared to the 8BL CH/P fabric, and similar spreading behavior to the CO fabric (maximum wetted radius 20 mm; spreading speed ~2.6 mm/s). These findings suggest that the presence of polyphenolic compounds and other hydrophilic constituents from the blackcurrant pomace extract disrupted the compactness of the chitosan/pectin assembly and introduced additional polar functional groups capable of interacting with water. Although the one-way transport capability remained positive (~120%), it was significantly lower than that of the 8BL CH/P fabric, pointing out a more balanced distribution of liquid between the two surfaces. The lower overall moisture management capacity value (0.38) compared to CO and 8BL CH/P reflects the combined influence of moderate absorption and directional transport. All these characteristics support the classification of 8BL CH-BC/P-BC fabric as a moisture-management fabric (Figure 7c).

3.5. Macromolecular Docking Analysis

Molecular docking simulations were conducted to assess the interaction strength and binding modes between the selected anthocyanin glycosides present in blackcurrant pomace extract and polysaccharides relevant to cotton fabric functionalization, namely cellulose, chitosan, and pectin. Four ligands were examined: cyanidin-3-O-glucoside, cyanidin-3-O-rutinoside, delphinidin-3-O-glucoside, and delphinidin-3-O-rutinoside. As summarized in Table 6, cyanidin-3-O-glucoside showed the most favorable binding free energy (ΔG) toward all three polysaccharide receptors compared with the other anthocyanin glycosides investigated. A comparative analysis of the receptors revealed that all ligands exhibited stronger binding affinity for chitosan and pectin than for cellulose, indicating that both polysaccharide layers exhibit greater interaction potential than the cellulose backbone. Based on the discussed results, cyanidin-3-O-glucoside was selected for an in-depth analysis of binding modes and intermolecular interactions with each polysaccharide receptor.

Docking of cyanidin-3-O-glucoside with cellulose resulted in a best-ranked binding pose characterized by a binding free energy of ΔG = −3.65 kcal/mol (Figure 8). In this configuration, the ligand was aligned along the cellulose chain and predominantly stabilized through hydrogen-bonding interactions between the cellulose hydroxyl groups and the phenolic and glycosidic hydroxyl groups of cyanidin-3-O-glucoside, with interaction distances ranging from approximately 1.8 to 3.0 Å. Additionally, carbon–hydrogen bonds were observed between the cellulose backbone and the aromatic system of cyanidin-3-O-glucoside, indicating the presence of weak yet stabilizing interactions. Furthermore, a Pi-Sigma hydrophobic interaction was also identified between the aromatic Pi-system of cyanidin-3-O-glucoside and the C–H bonds of cellulose, further contributing to complex stabilization. These combined interactions suggest that cellulose provides a hydrogen-bond-rich surface capable of associating with anthocyanins; however, the relatively limited number of close contacts is consistent with the lower predicted binding affinity compared with chitosan and pectin.

For chitosan, the top-ranked docking configuration of cyanidin-3-O-glucoside showed a stronger binding affinity compared to cellulose, with a free energy of ΔG = −4.31 kcal/mol (Figure 9). The binding mode was primarily governed by multiple hydrogen bonds between

the functional groups of chitosan and the hydroxyl groups of cyanidin-3-O-glucoside, with interaction distances ranging from approximately 1.9–3.1 Å. In addition, Pi-Sigma hydrophobic interaction was also observed between the aromatic rings of cyanidin-3-O-glucoside and the chitosan backbone, further contributing to complex stabilization. The presence of both hydrogen bonding and Pi-Sigma interactions suggests a favorable binding environment under acidic conditions, which is consistent with the enhanced interaction strength observed for chitosan compared to cellulose. In particular, the greater number and more favorable distribution of short-range hydrogen bonds appear to provide a more stable ligand-polymer complex than in the cellulose system.

Table 6. Binding free energies (ΔG) obtained from molecular docking of anthocyanin glycosides with polysaccharide receptors.

Cellulose	ΔG, kcal/Mol
cyanidin-3-O-glucoside	−3.65
cyanidin-3-O-rutinoside	−2.87
delphinidin-3-O-glucoside	−3.40
delphinidin-3-O-rutinoside	−2.92
Chitosan	
cyanidin-3-O-glucoside	−4.31
cyanidin-3-O-rutinoside	−3.34
delphinidin-3-O-glucoside	−4.00
delphinidin-3-O-rutinoside	−2.94
Pectin	
cyanidin-3-O-glucoside	−4.77
cyanidin-3-O-rutinoside	−3.72
delphinidin-3-O-glucoside	−4.56
delphinidin-3-O-rutinoside	−4.12

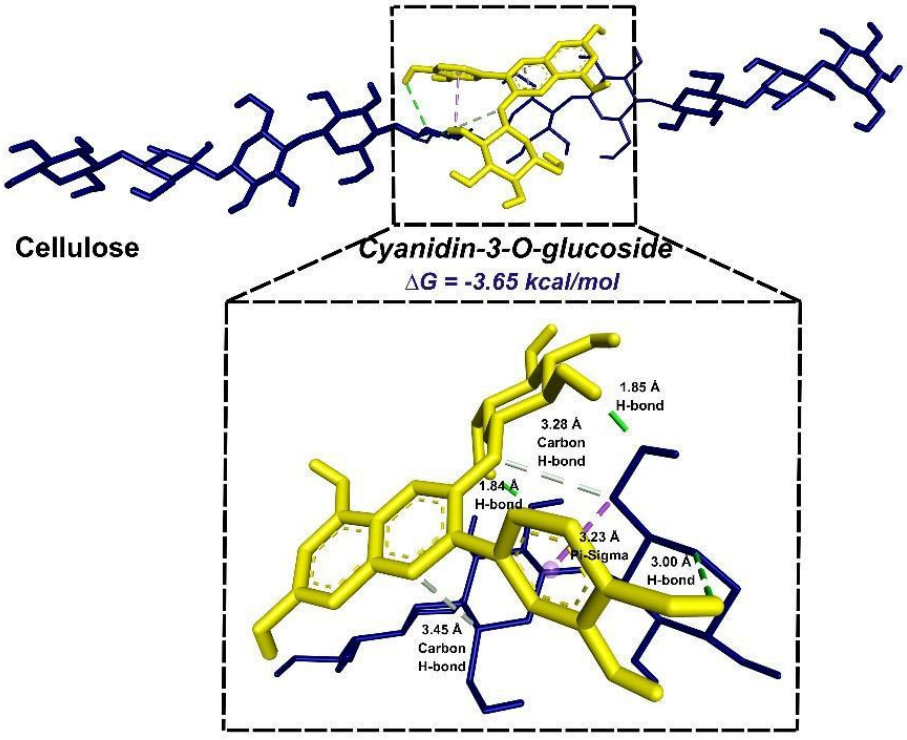


Figure 8. Molecular docking configuration of cyanidin-3-O-glucoside on cellulose.

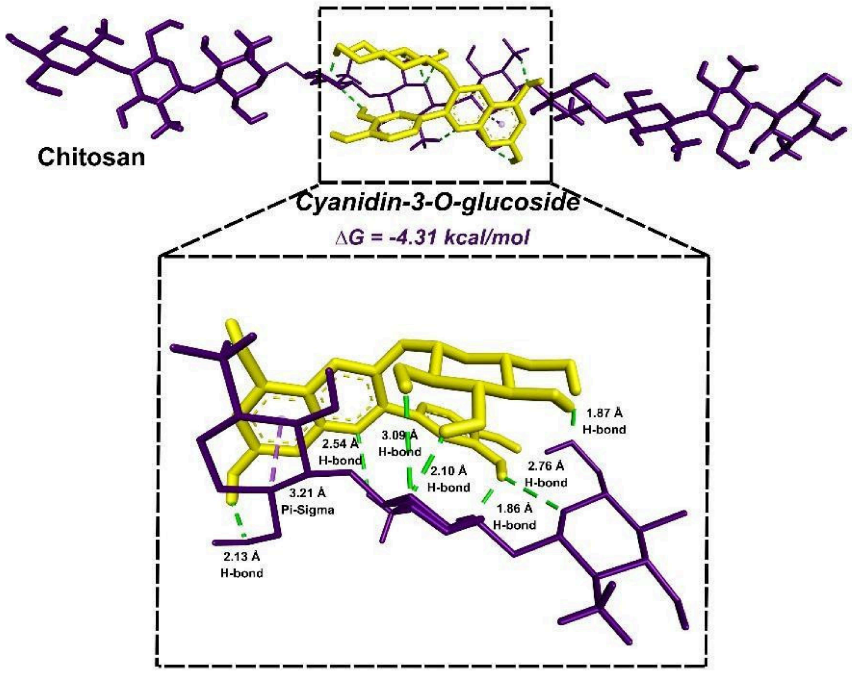


Figure 9. Molecular docking configuration of cyanidin-3-O-glucoside on chitosan.

The strongest binding interaction was predicted for the pectin–cyanidin-3-O-glucoside complex, with a calculated binding free energy of ΔG = −4.77 kcal/mol (Figure 10). In this system, the preferred binding pose was stabilized exclusively by an extensive network of hydrogen bonds, characterized by several short interaction distances ranging from 1.35 to 2.27 Å. No hydrophobic or Pi-Sigma interactions were detected in this complex, indicating that hydrogen bonding represents the dominant stabilizing force governing the association of cyanidin-3-O-glucoside with pectin. The high density of accessible carboxylate and hydroxyl groups in the pectin model likely enables more efficient and geometrically favorable hydrogen-bond formation, which is consistent with the highest binding affinity among the studied polysaccharides.

A clear and systematic increase in the binding affinity of cyanidin-3-O-glucoside was observed along the polymer sequence cellulose–chitosan–pectin, as indicated by progressively more negative binding free energies (−3.65, −4.31, and −4.77 kcal/mol, respectively). This hierarchical trend is significant from a functional perspective, as it suggests that successive functionalization of the polymer surface leads to stronger and potentially more durable immobilization of small bioactive molecules. Such an increase in affinity is expected to enhance overall surface functionality, especially in applications requiring prolonged retention and stability of active compounds.

The docking-derived interpretation presented in the current study aligns with recent experimental and computational studies showing that anthocyanin retention within polysaccharide matrices is strongly influenced by the type and geometry of noncovalent interactions. In a chitosan–anthocyanin colorimetric sensor system, molecular modeling identified electrostatic and hydrophobic contributions as the key stabilizing factors and reported a low-energy configuration (approximately −3 kcal/mol), along with π–cation contacts (at distances of approximately 4.14–4.29 Å) and a short π–sigma interaction (about 2.48 Å)

Taken together, these findings demonstrate that functional binding is governed not only by the absolute interaction distance range but also by the number, proximity, and cooperativity of short hydrogen bonds. While cellulose provides a fundamental interaction platform, the introduction of additional functional groups in chitosan and, more prominently, in pectin leads to a progressive increase in interaction density and strength. This

hierarchical progression from cellulose as the foundational layer, through chitosan, to pectin as the most interactive and accessible surface results in enhanced affinity and, consequently, increased surface functionality. The particularly high binding affinity observed for pectin is advantageous, as its abundant and readily accessible functional groups enable efficient and stable immobilization of small molecules. This structure–energy–distance relationship provides a molecular-level explanation for the observed improvement in performance with increasing chemical functionality of polysaccharide layers, thereby underscoring the critical role of polymer selection and surface design in the development of biofunctionalized interfaces.

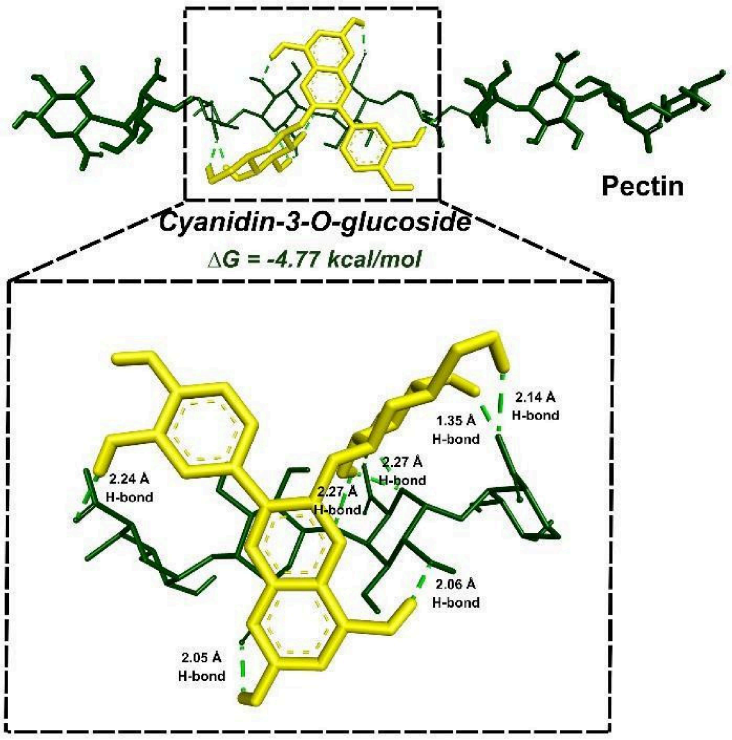


Figure 10. Molecular docking configuration of cyanidin-3-O-glucoside on pectin.

3.6. Potential Application of Selected Fabrics

The potential application of the investigated cotton fabrics can be proposed by integrating their antioxidant and antibacterial performance and liquid moisture management classification. Such a multifunctional approach is particularly relevant for developing medical, hygiene, and protective textile products where oxidative stress mitigation, microbial control, and moisture regulation are simultaneously required.

Fast-absorbing and quick-drying CO fabric with only 20% antioxidant activity and no antibacterial protection can be used for standard hospital bed linens. While it absorbs moisture quickly, the lack of antibacterial activity suggests it is best used in environments where frequent high-temperature laundering is guaranteed to compensate for the lack of inherent protective properties. CO fabric is also suitable for conventional comfort-oriented textile applications, including summer clothing or disposable hygiene substrates where rapid sweat absorption and evaporation contribute to thermal comfort, but no specific biofunctional performance is required. Its symmetric moisture distribution behavior also makes it appropriate for absorbent layers in multilayer textile assemblies, where moisture buffering rather than moisture pumping is desired.

The 8BL CH/P water penetration fabric offers low antioxidant activity (35%) and specifically strong protection against *E. coli* (98%). It is suitable for incontinence products since the high one-way transport ensures the wearer's skin remains dry by moving fluids

away from the body, while the polysaccharide-based coating provides a primary antibacterial barrier to prevent skin infections and odors associated with Gram-negative bacteria like *E. coli*. Also, 8BL CH/P fabric shows strong potential for protective and semi-occlusive medical textiles. For instance, it could be used as an intermediate layer in wound dressings or post-surgical textiles where controlled moisture migration away from the skin or wound interface is beneficial while maintaining a partial barrier against microbial penetration.

The moisture management 8BL CH-BC/P-BC fabric exhibits 100% antioxidant activity and 100% antibacterial protection against both *S. aureus* and *E. coli*. Owing to this multifunctional performance, the fabric represents a promising candidate for biofunctional wound dressings (e.g., for diabetic ulcers, pressure injuries, and burns) as well as for skin-contact therapeutic textiles. Specifically, its antioxidant capacity may contribute to the mitigation of oxidative stress at the wound site, thereby supporting the healing process, while its pronounced antibacterial activity can reduce the risk of infection and suppress the proliferation of odor-causing microorganisms. In addition, the favorable moisture-management properties help prevent tissue maceration by facilitating the transport of excess wound exudate away from the wound interface.

From a broader perspective, these results demonstrate that LbL polysaccharide-based finishing combined with bioactive extract incorporation enables application-driven tuning of cotton fabrics. The progression from comfort-oriented absorption (CO) through directional moisture control and partial bioactivity (8BL CH/P) to fully integrated moisture management and strong biofunctional protection (8BL CH-BC/P-BC) provides a versatile material platform suitable for next-generation medical and wellness textile systems.

4. Conclusions

This study presents a novel strategy for the development of biofunctional, biocompatible and skin-comfortable polysaccharide-based textiles through the incorporation of blackcurrant pomace extract into a chitosan/pectin LbL coating applied to the cotton fabric. Using response surface methodology, the extraction of bioactive compounds from blackcurrant pomace was optimized to maximize the yield of polyphenolic compounds (TPC = 36.04 mg GAE/g DW). The resulting extract is rich in flavonoids (TFC = 5.28 mg QE/g DW) and anthocyanins (a total content of 5.18 mg/g DW) and serves as a potent natural antioxidant and antimicrobial colorant.

The incorporation of the optimized extract into a chitosan/pectin LbL coating proved to be a highly effective approach for cotton fabric functionalization with bioactive compounds compared to the traditional extract exhaustion method. While untreated cotton and fabrics coated only with polysaccharides showed low antioxidant activity (27–39%) and negligible to excellent antibacterial activity (0–100) against *S. aureus* and *E. coli*, the incorporation of blackcurrant extract in the LbL assembly resulted in nearly 100% antioxidant activity, >92% cell viability, and excellent antibacterial activity (88–100%) against both tested bacteria. The number of deposited chitosan/pectin BLs plays a key role in controlling extract adsorption and, consequently, the intensity of fabric functionalization and coloration. The novelty of this study lies in integrating molecular docking analysis to elucidate, at the molecular level, the interactions between extract anthocyanins and all three polysaccharides (cellulose, chitosan, and pectin). Additionally, the performed functionalization protocols influenced the liquid moisture management behavior of the fabrics, leading to a balanced combination of absorption, spreading, and liquid transport, which is essential for maintaining skin comfort. The fabrics developed in this study are highly promising for conventional comfort-oriented textile applications; skin-contact therapeutic textiles; biofunctional wound dressings; and medical, hygiene, incontinence, and protective textile products.

Several limitations of the present study should be acknowledged. The long-term stability and durability under repeated laundering, wear, and extended storage conditions were not evaluated and warrant further investigation. Future studies should also focus on elucidating the release kinetics of the extract's bioactive compounds under physiologically relevant conditions, such as simulated sweat and wound exudates. Furthermore, the therapeutic efficacy of the developed fabrics should be validated through in vivo wound-healing studies to assess their ability to promote tissue regeneration and prevent infection.

Supplementary Materials: The following supporting information can be downloaded at https://www.mdpi.com/article/10.3390/polysaccharides7020072/s1, Table S1: ANOVA for final quadratic model, Table S2: Fit statistics for final quadratic model, and Figure S1: HPLC profile of blackcurrant pomace extract obtained under optimized conditions recorded at 520 nm. 1-delphinidin-3-O-glucoside, 2-delphinidin-3-O-rutinoside, 3-cyanidin-3-O-glucoside, and 4-cyanidin-3-O-rutinoside.

Author Contributions: Conceptualization, A.I.; methodology, A.I., M.Ć., A.P.I., T.L., A.T. and I.J.; investigation, A.I., M.Ć., A.P.I., T.L., A.T., X.-K.R. and I.J.; resources, A.I., M.Ć., A.T. and I.J.; writing—original draft preparation, A.I., M.Ć., A.P.I., T.L. and A.T.; writing—review and editing, X.-K.R. and I.J.; visualization, A.I., M.Ć. and T.L.; supervision, I.J.; project administration, A.I.; funding acquisition, A.I. All authors have read and agreed to the published version of the manuscript.

Funding: This research was funded by the European Commission through the Horizon Europe project POLICY ANSWERS (R&I POLICY making, implementation and support in the Western Balkans); the Ministry of Science, Technological Development and Innovation of the Republic of Serbia, grant numbers (451-03-33/2026-03/200287, 451-03-34/2026-03/200135, and 451-03-33/2026-03/200178); and International Sci-tech Cooperation Project under the "Innovation Yongjiang 2035" Key R&D Programme of Ningbo Municipality, grant number 2024H017.

Data Availability Statement: Data will be made available on request.

Acknowledgments: The authors thank Ana Vukoičić (Innovation Center of the Faculty of Technology and Metallurgy in Belgrade) for the determination of fabric antioxidant activity. The authors thank the Laboratory for Controlled Monitoring Cross-Linking Process for using the Drop Shape Analyzer DSA30S (KRÜSS GmbH, Germany) and the Moisture Management Tester MMT M290 (SDL Atlas, USA). This paper is based on work from COST Action ENFiber, CA24111, supported by COST (European Cooperation in Science and Technology).

Conflicts of Interest: The authors declare no conflicts of interest.

References

1. Luo, X.; Li, L. Chitosan's wide profile from fibre to fabrics. In *An Overview Chitin-Chitosan—Myriad Functionalities in Science and Technology*; Dongre, R.S., Ed.; IntechOpen: Rijeka, Croatia, 2018.
2. Massella, D.; Giraud, S.; Guan, J.; Ferri, A.; Salaün, F. Textiles for health: A review of textile fabrics treated with chitosan microcapsules. *Environ. Chem. Lett.* **2019**, *17*, 1787–1800. [CrossRef]
3. Freitas, A.S.; Oliveira, R.; Ribeiro, A.; Almeida-Aguiar, C. Biofunctional textiles: Antioxidant and antibacterial finishings of cotton with propolis and honey. *Int. J. Mol. Sci.* **2024**, *25*, 8034. [CrossRef] [PubMed]
4. Liu, S.; Sun, D. Bio-functional textiles. In *Handbook of Medical Textiles*; Bartels, V.T., Ed.; Woodhead Publishing: Cambridge, UK, 2011; pp. 336–359.
5. Massella, D.; Argenziano, M.; Ferri, A.; Guan, J.; Giraud, S.; Cavalli, R.; Barresi, A.A.; Salaün, F. Bio-functional textiles: Combining pharmaceutical nanocarriers with fibrous materials for innovative dermatological therapies. *Pharmaceutics* **2019**, *11*, 403. [CrossRef] [PubMed]
6. Szadkowski, B.; Śliwka-Kaszyńska, M.; Marzec, A. Bioactive and biodegradable cotton fabrics produced via synergic effect of plant extracts and essential oils in chitosan coating system. *Sci. Rep.* **2024**, *14*, 8530. [CrossRef] [PubMed]
7. Firmino, H.B.; Volante, E.K.T.S.; da Silva, A.C.P.; Scacchetti, F.A.P.; Lis, M.J.; Martí, M.; Saxena, S.; Tessaro, A.L.; Bezerra, F.M. β-cyclodextrin-modified cotton fabric for medical and hospital applications with photodynamic antibacterial activity using Methylene Blue. *Coatings* **2024**, *14*, 1100. [CrossRef]

8. Pucciarini, L.; Ianni, F.; Petesse, V.; Pellati, F.; Brighenti, V.; Volpi, C.; Gargaro, M.; Natalini, B.; Clementi, C.; Sardella, R. Onion (*Allium cepa* L.) akin: A rich resource of biomolecules for the sustainable production of colored biofunctional textiles. *Molecules* **2019**, *24*, 634. [CrossRef] [PubMed]
9. Puri, C.; Pucciarini, L.; Tiecco, M.; Brighenti, V.; Volpi, C.; Gargaro, M.; Germani, R.; Pellati, F.; Sardella, R.; Clementi, C. Use of a zwitterionic surfactant to improve the biofunctional properties of wool dyed with an onion (*Allium cepa* L.) skin extract. *Antioxidants* **2020**, *9*, 1055. [CrossRef] [PubMed]
10. Ivanovska, A.; Ćorović, M.; Lađarević, J.; Dimić-Mišić, K.; Jordanov, I. Chitosan/pectin layer-by-layer coatings enriched with strawberry pomace extract: A path to obtaining sustainable bio-colored healthcare cotton fabric. *Textiles* **2025**, *5*, 68. [CrossRef]
11. Petkovska, J.; Geskovski, N.; Marković, D.; Dimova, V.; Mirakovski, D.; Radetić, M.; Jordanov, I. Chitosan-pectin multilayer coating with anthocyanin grape dye as pH indicating wound dressing: Synthesis and characterization. *Carbohydr. Polym. Technol. Appl.* **2024**, *7*, 100438. [CrossRef]
12. Martí, M.; Martínez, V.; Lis, M.J.; Coderch, L. Mathematical models for drug delivery from textile. *J. Ind. Text.* **2021**, *50*, 1225–1238. [CrossRef]
13. Nawawi, N.I.M.; Khushairi, N.A.A.A.; Ijod, G.; Azman, E.M. Extraction of anthocyanins and other phenolics from dried blackcurrant (*Ribes nigrum* L.) pomace via ultrasonication. *Sustain. Chem. Environ.* **2025**, *9*, 100208. [CrossRef]
14. Ejaz, A.; Waliat, S.; Afzaal, M.; Saeed, F.; Ahmad, A.; Din, A.; Ateeq, H.; Asghar, A.; Shah, Y.A.; Rafi, A.; et al. Biological activities, therapeutic potential, and pharmacological aspects of blackcurrants (*Ribes nigrum* L): A comprehensive review. *Food Sci. Nutr.* **2023**, *11*, 5799–5817. [CrossRef] [PubMed]
15. Martí, M.; Martínez, V.; Lis, M.J.; Valldeperas, J.; de la Maza, A.; Parra, J.L.; Coderch, L. Gallic acid vehiculized through liposomes or mixed micelles in biofunctional textiles. *J. Text. Inst.* **2014**, *105*, 175–186. [CrossRef]
16. Petrov Ivanković, A.; Ćorović, M.; Milivojević, A.; Simović, M.; Banjanac, K.; Veljković, M.; Bezbradica, D. Berries pomace valorization: From waste to potent antioxidants and emerging skin prebiotics. *Int. J. Fruit Sci.* **2024**, *2*, 85–101. [CrossRef]
17. Petrov Ivanković, A.; Milivojević, A.; Ćorović, M.; Simović, M.; Banjanac, K.; Jansen, P.; Vukoičić, A.; van den Bogaard, E.; Bezbradica, D. In vitro evaluation of enzymatically derived blackcurrant extract as prebiotic cosmetic ingredient: Extraction conditions optimization and effect on cutaneous microbiota representatives. *Chem. Biol. Technol. Agric.* **2023**, *10*, 125. [CrossRef]
18. Pavun, L.; Spasojević, D.; Ivanovska, A.; Lađarević, J.; Milenković, M.; Uskoković-Marković, S. Characterization of tea water extracts and their utilization for dyeing and functionalization of fabrics of different chemical compositions. *Maced. J. Chem. Chem. Eng.* **2023**, *42*, 263–273. [CrossRef]
19. Ugrinović, V.; Simović, A.; Ćorović, M.; Mihajlovski, K.; Lađarević, J.; Bajat, J.; Ivanovska, A. Valorization of Aronia melanocarpa Pomace: A Sustainable Source of Bioactive Compounds for Developing Colored Healthcare Textiles, Biomedical Hydrogels, and Green Corrosion Inhibitor. *Sustain. Chem.* **2025**, *6*, 46. [CrossRef]
20. Ivanovska, A.; Petrović, A.; Lazarević-Pašti, T.; Ilic-Tomic, T.; Dimić-Mišić, K.; Lađarević, J.; Bradić, J. Development of bioactive cotton, wool, and silk fabrics functionalized with *Origanum vulgare* L. for healthcare and medical applications: An in vivo study. *Pharmaceutics* **2025**, *17*, 856. [CrossRef] [PubMed]
21. *ISO 3071:2020*; Textiles—Determination of pH of Aqueous Extract, 4th ed. International Organization for Standardization (ISO): Geneva, Switzerland, 2020.
22. *AATCC TM 195-2017*; Liquid Moisture Management Properties of Textile Fabrics. American Association of Textile Chemists and Colorists: Durhamk, NC, USA, 2017.
23. *ISO 19403-6:2024*; Paints and Varnishes—Wettability—Part 6: Measurement of Dynamic Advancing and Receding Angle by Changing the Volume of a Drop. International Organization for Standardization: Geneva, Switzerland, 2024.
24. Grant, O.C.; Wentworth, D.; Holmes, S.G.; Kandel, R.; Sehnal, D.; Wang, X.; Xiao, Y.; Sheppard, P.; Grelsson, T.; Coulter, A.; et al. Generating 3D Models of Carbohydrates with GLYCAM-Web. *Nat. Methods* **2026**, *23*, 720–723. [CrossRef] [PubMed]
25. Biovia, D.S. *Discovery Studio*; Dassault Systèmes BIOVIA: San Diego, CA, USA, 2016.
26. Hanwell, M.D.; Curtis, D.E.; Lonie, D.C.; Vandermeersch, T.; Zurek, E.; Hutchison, G.R. Avogadro: An advanced semantic chemical editor, visualization, and analysis platform. *J. Cheminform.* **2012**, *4*, 17. [CrossRef] [PubMed]
27. Morris, G.M.; Huey, R.; Lindstrom, W.; Sanner, M.F.; Belew, R.K.; Goodsell, D.S.; Olson, A.J. AutoDock4 and AutoDockTools4: Automated docking with selective receptor flexibility. *J. Comput. Chem.* **2009**, *30*, 2785–2791. [CrossRef] [PubMed]
28. Zerajić, S.A.; Savić Gajić, I.M.; Savić, I.M.; Nikolić, G.S. Kvašenje i namakanje bolničkog zaštitnog tekstila. *Adv. Technol.* **2019**, *8*, 10–18.
29. Brahmi, F.; Mateos-Aparicio, I.; Garcia-Alonso, A.; Abaci, N.; Saoudi, S.; Smail-Benazzouz, L.; Guemghar-Haddadi, H.; Madani, K.; Boulekbache-Makhlouf, L. Optimization of conventional extraction parameters for recovering phenolic compounds from potato (*Solanum tuberosum* L.) peels and their application as an antioxidant in yogurt formulation. *Antioxidants* **2022**, *11*, 1401. [CrossRef] [PubMed]
30. Rubinskiene, M.; Jasutiene, I.; Venskutonis, P.R.; Viskelis, P. HPLC determination of the composition and stability of blackcurrant anthocyanins. *J. Chromatogr. Sci.* **2005**, *43*, 478–482. [CrossRef] [PubMed]

31. Šimerdová, B.; Bobríková, M.; Lhotská, I.; Kaplan, J.; Křenová, A.; Šatínský, D. Evaluation of anthocyanin profiles in various blackcurrant cultivars over a three-year period using a fast HPLC-DAD method. *Foods* **2021**, *10*, 1745. [CrossRef] [PubMed]
32. Wang, Z.; Yan, Y.; Zhang, Z.; Li, C.; Mei, L.; Hou, R.; Liu, X.; Jiang, H. Effect of chitosan and its water-soluble derivatives on antioxidant activity. *Polymers* **2024**, *16*, 867. [CrossRef] [PubMed]
33. Chatterjee, N.S.; Panda, S.K.; Navitha, M.; Asha, K.K.; Anandan, R.; Mathew, S. Vanillic acid and coumaric acid grafted chitosan derivatives: Improved grafting ratio and potential application in functional food. *J. Food Sci. Technol.* **2015**, *52*, 7153–7162. [CrossRef]
34. Xie, W.; Xu, P.; Liu, Q. Antioxidant activity of water-soluble chitosan derivatives. *Bioorg. Med. Chem. Lett.* **2001**, *11*, 1699–1701. [CrossRef] [PubMed]
35. Wang, W.; Ma, X.; Jiang, P.; Hu, L.; Zhi, Z.; Chen, J.; Ding, T.; Ye, X.; Liu, D. Characterization of pectin from grapefruit peel: A comparison of ultrasound-assisted and conventional heating extractions. *Food Hydrocoll.* **2016**, *61*, 730–739. [CrossRef]
36. Nanashima, N.; Horie, K.; Maeda, H.; Tomisawa, T.; Kitajima, M.; Nakamura, T. Blackcurrant anthocyanins increase the levels of collagen, elastin, and hyaluronic acid in human skin fibroblasts and ovariectomized rats. *Nutrients* **2018**, *10*, 495. [CrossRef] [PubMed]
37. Nosal, B.M.; Sakaki, J.R.; Mofrad, M.D.; Macdonald, Z.; Mahoney, K.J.; Thornton, S.N.; Patel, D.; Drossman, J.; Lee, E.C.-H.; Chun, O.K. Blackcurrant anthocyanins improve blood lipids and biomarkers of inflammation and oxidative stress in healthy women in menopause transition without changing body composition. *Biomedicines* **2023**, *11*, 2834. [CrossRef] [PubMed]
38. Puca, V.; Marulli, R.Z.; Grande, R.; Vitale, I.; Niro, A.; Molinaro, G.; Prezioso, S.; Muraro, R.; Di Giovanni, P. Microbial species isolated from infected wounds and antimicrobial resistance analysis: Data emerging from a three-years retrospective study. *Antibiotics* **2021**, *10*, 1162. [CrossRef] [PubMed]
39. Dahal, A.; Chang, W.C.; Johansson, E.; Grashel, B.; Morgan, D.; Williams, L.; Hammonds, M.; Sachdeva, S.; Spagna, D.; Satish, L.; et al. Skin *Staphylococcus aureus* detection and relationship to atopic dermatitis outcomes using culture and metagenomic sequencing. *Sci. Rep.* **2025**, *15*, 17606. [CrossRef] [PubMed]
40. Cholewa, K.; Kurtyka, P.; Szuber-Dynia, A.; Kapis, A.; Gawlikowski, M. Local Infections Associated with Ventricular Assist Devices: Materials-Related Challenges and Emerging Solutions. *Materials* **2025**, *18*, 4541. [CrossRef] [PubMed]
41. Yan, D.; Li, Y.; Liu, Y.; Li, N.; Zhang, X.; Yan, C. Antimicrobial properties of chitosan and chitosan derivatives in the treatment of enteric infections. *Molecules* **2021**, *26*, 7136. [CrossRef] [PubMed]
42. Aprodu, I.; Chitescu, C.L.; Grigore-Gurgu, L.; Dumitrașcu, L. Investigation of the antioxidant and antimicrobial properties of ultrasound-assisted extracted phenolics from *Aronia melanocarpa* pomace. *Appl. Sci.* **2025**, *15*, 7070. [CrossRef]
43. *ISO 10993-5:2009*; Biological Evaluation of Medical Devices—Part 5: Tests for In Vitro Cytotoxicity. International Organization for Standardization (ISO): Geneva, Switzerland, 2009.
44. Gozel Yavuz, G.T.; Yilmaz, E. Comparative evaluation of ultrasound-assisted and conventional extraction methods for anthocyanin recovery and antioxidant potential from blackcurrant. *Food Meas.* **2026**, *20*, 1465–1481. [CrossRef]
45. Brennan, E.; Pressete, C.G.; Mohammadi, N.; Antunes, L.M.G.; Shang, Q.; Chen, J.; Bennett, J.; Franchin, M.; Granato, D. Ultrasound-assisted recovery of blackcurrant press cake anthocyanins: Antioxidant and anti-inflammatory properties, bioaccessibility, and application in functional gummies. *Food Chem. X* **2025**, *26*, 102285. [CrossRef] [PubMed]
46. Khalaf, D.; Pradal, D.; Dimitrov, K. Multi-criteria optimization including environmental impacts of ultrasound-assisted extraction of phenolic antioxidants from blackcurrant pomace by-product. *Chem. Eng. Process. Process Intensif.* **2024**, *204*, 109935. [CrossRef]
47. Cîrstea, N.; Nour, V.; Corbu, A.R.; Codină, G.G. Blackcurrant pomace extract as a natural antioxidant in Vienna sausages reformulated by replacement of pork backfat with emulsion gels based on high oleic sunflower and flaxseed oils. *Gels* **2024**, *10*, 534. [CrossRef] [PubMed]
48. Meremäe, K.; Raudsepp, P.; Rusalepp, L.; Anton, D.; Bleive, U.; Roasto, M. In vitro antibacterial and antioxidative activity and polyphenolic profile of the extracts of chokeberry, blackcurrant, and rowan berries and their pomaces. *Foods* **2024**, *13*, 421. [CrossRef] [PubMed]
49. Trajković, M.; Kitić, D.; Mihajilov-Krstev, T.; Šavikin, K.; Ranđelović, M.; Milutinović, M.; Branković, S.; Kitić, N.; Miladinović, B. Antimicrobial activity evaluation of black currant (*Ribes nigrum* L.) variety Čačanska crna juice and extract. *AFMN Biomed.* **2023**, *40*, 208–216. [CrossRef]
50. Ionescu, C.; Samide, A.; Tigae, C. Trend in detection of anthocyanins from fresh fruits and the influence of some factors on their stability impacting human health: Kinetic study assisted by UV–Vis spectrophotometry. *Antioxidants* **2025**, *14*, 227. [CrossRef] [PubMed]
51. Yasukawa, A.; Chida, A.; Kato, Y.; Kasai, M. Dyeing silk and cotton fabrics using natural blackcurrants. *Text. Res. J.* **2017**, *87*, 2379–2387. [CrossRef]
52. Čorak, I.; Tarbuk, A.; Dekanić, T.; Sikorski, D.; Draczyński, Z. The functionalization of activated polyester fabrics with chitosan—Changes in zeta potential and moisture management. *Materials* **2024**, *17*, 5987. [CrossRef] [PubMed]

53. Atlas, S.D.L. *M290 Moisture Management Tester: Instruction Manual*; Rev. 1.4 (06/18); SDL Atlas Inc.: Charlotte, NC, USA, 2010. Available online: www.sdlatlas.com (accessed on 3 March 2026).
54. Tarbuk, A.; Flinčec Grgac, S.; Dekanić, T. Wetting and wicking of hospital protective textiles. *Adv. Technol.* **2019**, *8*, 5–15. [CrossRef]
55. Tarbuk, A.; Grancarić, A.M.; Begović, S.; Dekanić, T. Interfacial Phenomena of Cotton/Polyester Blended Fabric Modified with Enzyme and Chitosan. *Polymers* **2026**, *18*, 867. [CrossRef] [PubMed]

Disclaimer/Publisher's Note: The statements, opinions and data contained in all publications are solely those of the individual author(s) and contributor(s) and not of MDPI and/or the editor(s). MDPI and/or the editor(s) disclaim responsibility for any injury to people or property resulting from any ideas, methods, instructions or products referred to in the content.